eScience 5 (2025) 100281

Contents lists available at ScienceDirect

eScience

journal homepage: www.keaipublishing.com/en/journals/escience

Review

Heterogeneous structure design for stable Li/Na metal batteries: Progress and prospects

Hongyang Chen [a], Junxiong Wu [a,*], Manxian Li [a], Jingyue Zhao [a], Zulin Li [a], Manxi Wang [a], Xuan Li [a], Chuanping Li [a], Xiaochuan Chen [a], Xiaoyan Li [a,*], Yiu-Wing Mai [b,*], Yuming Chen [a,*]

[a] Engineering Research Center of Polymer Green Recycling of Ministry of Education, Fujian Key Laboratory of Pollution Control & Resource Reuse, College of Environmental and Resource Sciences and College of Carbon Neutral Modern Industry, Fujian Normal University, Fuzhou 350000, China
[b] Department of Mechanical Engineering, The Hong Kong Polytechnic University, Hung Hom, Kowloon, Hong Kong, China

HIGHLIGHTS

- The fundamentals of metal dendrite growth are outlined.
- The design concepts, preparations, and applications of heterogeneous structures for Li/Na metal batteries are discussed.
- Challenges and future perspectives on the design of heterogeneous structures for metal batteries are presented.

GRAPHICAL ABSTRACT

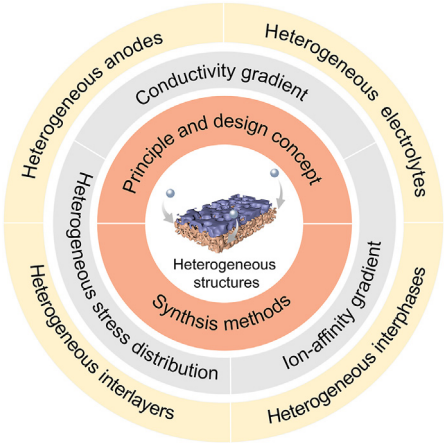

ARTICLE INFO

Keywords:
Li/Na metal batteries
Heterogeneous structures
Dendrites
Hosts
Interlayers

ABSTRACT

The growth of dendrites in Li/Na metal batteries is a multifaceted process that is controlled by several factors such as electric field, ion transportation, temperature, and pressure. Rational design of battery components has become a viable approach to address this challenge. Among the various design strategies, heterogeneous structures have been demonstrated to be effective in mitigating uneven metal deposition by reducing the local current density and regulating the deposition sites. In this review, we discuss comprehensively the underlying principles and factors that influence dendrite growth, as well as the synthesis approaches for heterogeneous structures. Furthermore, we provide an overview of the diverse applications of heterogeneous structures in battery components. Finally, we highlight existing challenges and future directions for the use of heterogeneous structures in regulating metal deposition.

* Corresponding authors.
E-mail addresses: jwuba@fjnu.edu.cn (J. Wu), xiaoyanli1985@126.com (X. Li), yw.mai@polyu.edu.hk (Y.-W. Mai), yumingc126@126.com (Y. Chen).

https://doi.org/10.1016/j.esci.2024.100281
Received 4 January 2024; Received in revised form 19 April 2024; Accepted 20 May 2024
Available online 23 May 2024

1. Introduction

Energy is an indispensable resource for human society. However, the exploitation of fossil fuels has resulted in detrimental impacts on the environment, necessitating the development and adoption of clean energy sources [1]. Concurrently, the demand for highly efficient energy storage devices has intensified. Lithium-ion batteries (LIBs), which were invented in the 1990s, have revolutionized the field of portable devices by enhancing their stability and lifespan, and are considered one of the most promising technologies for storing new energy sources [2,3]. Hitherto, LIBs have performed a critical role in the development of portable devices [4–6], electrification of automobiles [7,8], and grid-scale energy storage [9]. However, the theoretical energy densities of LIBs are approaching their limit, falling short of the ever-increasing demand for state-of-the-art electronic devices and electric vehicles [10]. In this regard, rechargeable lithium (Li) metal batteries with higher energy densities have been revisited with widespread interest [11]. Metallic Li, with its high capacity (3860 mAh g^{-1}) and low redox potential (−3.04 V *vs.* SHE), is dubbed the "holy grail" anode [12,13]. Additionally, sodium (Na) metal batteries have attracted increasing attention owing to their high capacities and abundant resources [3]. However, uneven deposition of metal ions on the anode side leads to notorious dendrite growth, which has become a most challenging issue in the development and commercialization of Li/Na metal batteries [14, 15]. The uncontrollable growth of dendrites not only creates "dead metal", but also leads to battery short circuits if the dendrites pierce the separator [16–18]. Hence, the dendrite growth issue must be resolved to enhance the safety and cycling performance of Li/Na metal batteries.

The uncontrollable growth of metal dendrites in rechargeable Li/Na metal batteries is a complex issue that arises from three main factors: (1) high local current density on the anode surface, (2) uneven metal ion distribution within the cell, and (3) repeated fracture of the solid electrolyte interphase (SEI) that continuously exposes the anode to the electrolyte [19–21]. The SEI forms on the anode surface can ideally prevent side reactions between the anode and the electrolyte. Unfortunately, the dramatic volume change of Li/Na metal anodes during charging and discharging causes the SEI to crack. The re-exposure of fresh metal to the electrolyte not only depletes the electrolyte and the anode but also generates non-uniform SEI, which incurs uneven metal deposition [22–24]. The growth of dendrites is a multifactorial process which has been explained using the well-established "Sand's time" [25] and space charge theory [26]. Researchers have also identified other influencing factors that dictate the metal deposition behavior. For example, Gao et al. investigated the growth of dendrites from a thermodynamic perspective and concluded that the energy needed for nucleation is higher at lower temperatures [27]. When the temperature increases, the nucleation overpotential decreases, yielding a larger nucleation radius and lower nucleation densities. Fang et al. studied the effect of external forces on the inhibition of dendrite growth [28]. By applying an optimized stacking pressure, the deposited Li presented a dense structure, thus mitigating dendrite growth. Since the irregular deposition of metals is affected by multiple factors, new materials with sophisticated structures should be developed to enable better metal deposition and extend the lifespan of Li/Na metal batteries.

To mitigate dendrite growth in Li/Na metal batteries, a variety of strategies have been studied: (1) creating new liquid or solid-state electrolytes (SSEs) to stabilize the electrode–electrolyte interfaces [29–33], (2) constructing artificial SEIs or interlayers on the anode to minimize side reactions [34,35], (3) developing three-dimensional (3D) hosts to accommodate the volume changes during metal deposition/dissolution [36–38], (4) modifying the separators to achieve higher mechanical strength and faster ion transport [39,40], and (5) optimizing the operation parameters, including working temperature, external pressure, and applied current [41,42]. However, the homogeneous design of components does not address the concentration gradient of ions and the distribution of electric field in the direction perpendicular to the anode, which is the main cause of dendrite growth. In the context of 3D metal hosts, it is evident that dendrite growth predominantly occurs on the upper surface of conductive hosts (e.g., metallic and carbon-based materials), because of the higher ion concentration and lower transport resistances at that location [43]. In dielectric hosts, the deposition/dissolution process is limited to only a few localized areas, which hampers the effective utilization of the host's pore space. Consequently, the adoption of 3D homogeneous hosts fails to sufficiently regulate the deposition/dissolution behavior, thus hindering the attainment of highly reversible Li/Na metal anodes. To circumvent this issue, heterogeneous designs for batteries have been explored, which include heterogeneous structures that vary in mechanical strength, pore size/porosity, and heterogeneous components that change phases and concentrations [44–46]. These designs help to mitigate dendrite growth by redistributing the metal ion flux and electric field, thus enabling better control over metal deposition. Although many reviews have provided viable approaches to mitigate dendrite growth [47,48], a timely and comprehensive review is essential to highlight the latest advances and provide new ideas on adopting heterogeneous structures in Li/Na metal batteries.

This review presents recent progress made in the development of heterogeneous structures in battery components, e.g., host, interlayer, electrolyte, and SEI, to prevent dendrite growth in batteries (Fig. 1). The fundamentals of metal dendrite growth are first outlined, providing the basis for the construction of vertically heterogeneous structures. In addition, various designs and preparation methods for vertically heterogeneous structures are described and a summary of their regulation mechanisms is given. Finally, the challenges and limitations of heterogeneous structures are discussed, and potential avenues for promoting their applications in high-energy-density Li/Na metal batteries are presented.

2. Fundamentals of metal dendrite growth

The morphology of heterogeneous metal deposition can be classified into three types: mossy-like, whisker-like, and dendrite-like [49]. These distinct growth patterns are attributed to various factors (Fig. 2a). The growth of mossy-like and whisker-like metal is mainly influenced by the stress field. During the initial stage of metal deposition, irregular metal growth is inhibited by the SEI layer, which grows faster than the metal deposition rate. As metal deposition continues, the stress builds up in the SEI until it ruptures at a threshold point. This exposes the conductive metal underneath the SEI to the electrolyte, leading to preferential metal deposition, and hence forming metal whiskers. The growth pattern of mossy metal is like that of metal whiskers, but it occurs at a current density higher than metal whiskers and lower than metal dendrites. For dendrite-like growth, it is mainly controlled by the ionic concentration and electric fields, which significantly affect metal nucleation (e.g., size and distribution density of nucleation sites) and deposition (e.g., deposition rate and morphology). In this section, we present two most famous theories, *viz.*, Sand's time model and space charge theory, that are used to predict metal dendrite formation. We also summarize the factors that influence dendrite growth, including nucleation behaviors, SEI properties, stress, and temperature, and explain how they affect metal deposition.

2.1. Theoretical models for metal deposition

Much work has been done to simulate and optimize the ions migration and electric field distribution behavior, among them, two main models are used to analyze the effect of ionic and electric fields on metal deposition, i.e., Sand's time theory and space charge theory.

In 1901, Sand concluded that, given the presence of an ion A, the ion would be released at the minimum electromotive force at the electrode; other particles that require a higher potential only appear when the concentration of ion A drops to zero [25]. Sand's time is given by:

$$t_s = \pi D\left(\frac{Z_c e C_0}{2J}\right)\left(\frac{\mu_a + \mu_b}{\mu_a}\right) \quad (1)$$

where D is the ambipolar diffusion coefficient, e electronic charge, Z_c charge number of electro-plating cations, C_0 initial salt concentration, J effective electrode current density, μ_a and μ_b the mobilities of anion and cation, respectively. Thus, based on Eq. (1), the effective current density greatly affects the time of dendrite formation.

In 2001, Brissot et al. proposed another model, in which the overall salt content in the cell is considered a constant value since the cathode releases Li ions to compensate for the loss on the anode during the charging process [49]. On the movement of anions toward the cathode, a linear-changing Li-salt concentration gradient occurs after polarization; and the Li-ion concentration becomes [49]:

$$C_+ = C_0 - \frac{\mu_a}{\mu_a + \mu_b}\frac{Jl}{FD} \quad (2)$$

where C_+ is the surface concentration of the anion, F Faraday constant, l diffusion distance of cations, and $l = \sqrt{t_D D_C}$, t_D is the diffusion time of the cations. Note that the significance of both cation and anion behaviors on dendrite growth during Li plating is highlighted in this theory.

Furthermore, Chazalviel proposed the space charge theory, which supports and supplements Sand's time theory. Fig. 2b displays two defined regions. One is the bulk electrolyte region (Region I), and the other is the electrolyte and electrode interface region (Region II) [50,51]. When the current density exceeds the critical value, the anions in Region II decrease significantly, giving space charge, which leads to explosive dendrite growth. The critical current density J^* is given below by Ref. [26]:

$$J^* = \frac{2eC_0 D}{t_a L} \quad (3)$$

$$t_a = \frac{\mu_a}{\mu_a + \mu_c} \quad (4)$$

where L is the inter-electrode distance. In addition, the same group predicted the growth rate of dendrites from Ref. [51]:

$$v_a = -\mu_a E_0 \quad (5)$$

where E_0 is electric field intensity in the neutral region of the electrolyte. Monroe and Newman challenged the above constant-growth-rate theory by demonstrating that the distribution of ionic concentration and electric fields on dendrite tips continuously varied during growth [52], and the growth rate would change over time. In this context, it is possible to prevent effectively dendrite growth by reducing the current density on the tip.

The abovementioned theories provide a solid understanding of the growth mechanism of tree-like metal dendrites. However, these theories also have certain limitations. Firstly, these models overlook the inhomogeneities of the ionic concentration field and electric field on the anode surface in real-life scenarios. Secondly, they do not provide precise explanations for the growth mechanisms of whisker-like and mossy-like metal deposition. Nor do they consider the influence of the nascent SEI layer formed spontaneously on the surface of Li/Na metals. In the following subsection, we will provide a concise overview of how other influencing factors, for example, nucleation states of Li/Na metals, properties of SEI layer, stress, and temperature, impact the deposition of Li/Na metals and subsequently control the battery performance.

2.2. Factors influencing the electrochemical deposition of metals

2.2.1. Nucleation behaviors

Nucleation is the initial step for metal deposition. In rechargeable cells, metal plating usually begins with heterogeneous nucleation on the surface of pristine metal or other substrates. The substrate's characteristics, such as its composition, size, morphology, and surface chemistry, all have a direct impact on the distribution of concentration/electric fields around the substrate, thereby influencing the metal nucleation and subsequent growth behaviors. Ely and Garcia summarized the electrochemical deposition of metal containing five regimes. These include the nucleation suppression regime, long incubation time regime, short incubation time regime, early growth regime, and late growth regime, which are used to explain the initial deposition behavior of Li metal by numerical simulation [53]. In the nucleation suppression regime, embryos are unstable and tend to redissolve in the electrolyte. The overpotential dictates the ensuing long incubation time and short incubation time regimes, which produce very broad and narrow nuclei size distributions, respectively. Finally, thermodynamically and kinetically stable nuclei grow, and the morphology and microstructure of the deposited metal evolve. Wood et al. used operando video microscopy to characterize the morphology evolution of metallic Li, giving a complete understanding of nucleation kinetics by combining the morphology evolution with the voltage variation [54]. Fig. 2c illustrates that the voltage rises to a local maximum immediately at the beginning of the charging process and then gradually falls back to a platform as time elapses. The sharp inflection occurs because nucleation requires an additional energy barrier (Fig. 2d). After the nucleation of metal on the anode, Li ions prefer to deposit on existing nuclei rather than a new one.

Based on thermodynamics, the formation of dendrites is highly related to the surface energy and diffusion energy barrier of the metal on the substrate [55]. High surface energy inhibits the vertical growth of the metal, hence reducing the probability of dendrite growth. Meanwhile, the diffusion energy barrier of metal atoms on the substrate also has a

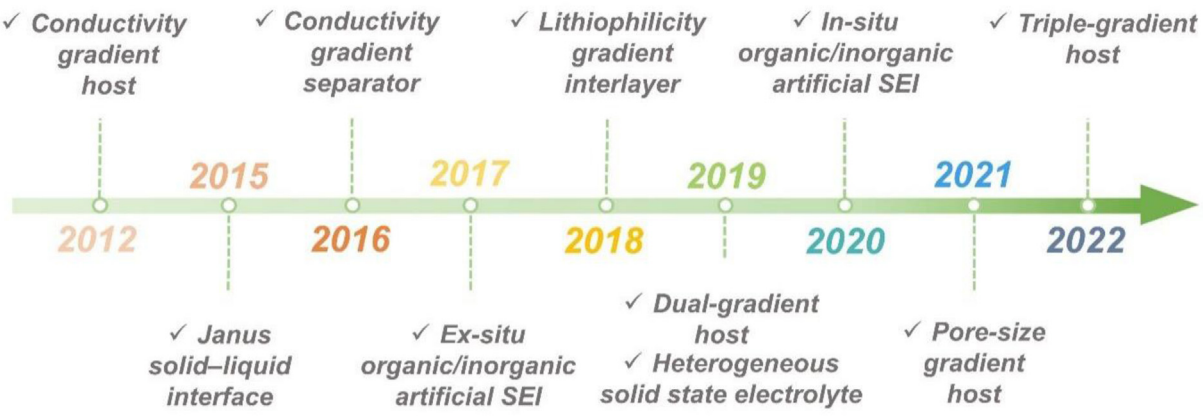

Fig. 1. Development of heterogeneous structures for Li/Na metal batteries.

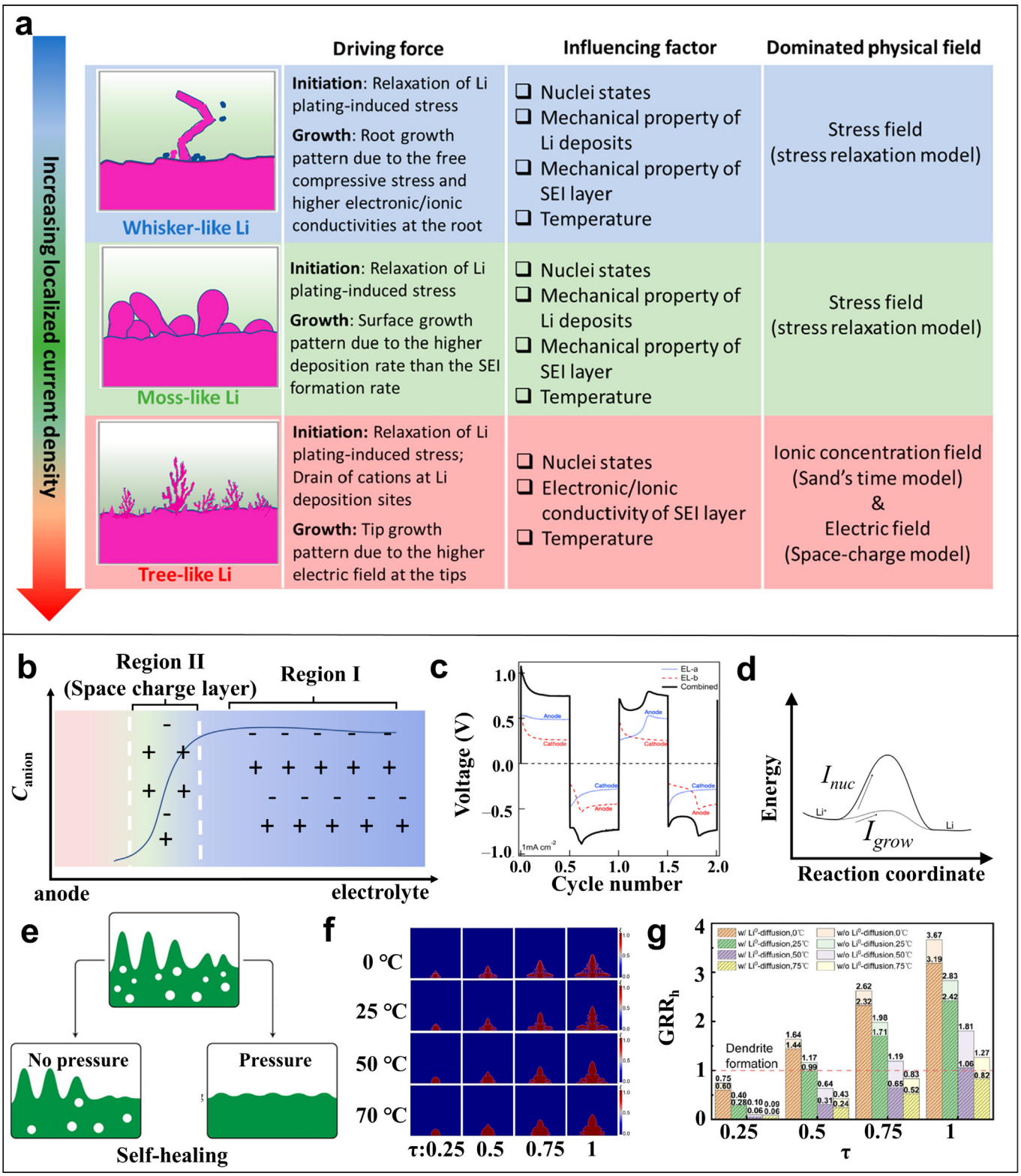

Fig. 2. (a) Summary of the driving force, influencing factor, and dominated physical fields for the different likes of Li deposition. Reproduced with permission from Ref. [49]. Copyright 2021 American Chemical Society. (b) Schematic illustration of a typical space charge layer in metal batteries, in which C_{anion} is the concentration of anions. (c) Three-electrode measurements showing the cell polarization contributions from each electrode. (d) Schematic representation of the difference in activation barriers in the cathodic (electrodeposition) process involving nucleation (labeled by 'nuc') and growth (labeled by 'grow'). Reproduced with permission from Ref. [54]. Copyright 2016 American Chemical Society. (e) Schematic showing the external pressure alleviates Li dendrite formation. Reproduced with permission from Ref. [72]. Copyright 2016 Wiley-VCH GmbH. (f) Snapshots of dendrite morphology for the phase-field model coupled with the atom diffusion model with τ at different temperatures, τ is the normalized plating time calculated by $\tau = t/t^*$, where t is the plating time and t^* is the time at the plating capacity of 0.2 mAh cm^{-2}. (g) The vertical growth rate ratio (GRR_h) variation with τ at different temperatures. Reproduced with permission from Ref. [73]. Copyright 2023 American Chemical Society.

critical role in dictating their deposition. A high diffusion energy barrier means the metal atoms tend to aggregate at specific sites, thereby inducing uneven deposition on the substrate [56]. Thus, researchers have designed substrates with high surface energy and low diffusion energy barrier to cope with dendrites.

Nucleation overpotential is a critical indicator to evaluate the difficulty of metal nucleation on different substrates and is closely linked to the lithiophilicity of the substrate [57–59]. It has been observed that Cu exhibits poor lithiophilicity and a large overpotential for Li nucleation owing to the significant difference in their lattice structures. In comparison, silver and gold have negligible nucleation potential and plating potential because these substrates can form Li alloys that have a similar lattice structure to pure Li metal with excellent lithiophilicity [60]. Besides metallic substrates, carbon-based materials are promising metal hosts because of their low-cost, lightweight, and high electrical conductivity [61]. However, Xu et al. discovered that the affinity between Li atoms and bulk Li is stronger than that between Li atoms and pure carbon substrates using density functional theory (DFT), supported by the larger $E_{Li–Li}$ (1.443 eV) than $E_{Li–C}$ (1.147 eV) [62]. Therefore, as will be discussed later, surface defects and lithiophilic seeds have been designed on carbonaceous materials in order to reduce the nucleation overpotential and homogenize Li deposition.

2.2.2. SEI

SEI is an electrically insulating and ionically conductive passivation layer that forms on the electrode surface through electrolyte decomposition [63]. For Li/Na metals, the SEI layer forms immediately upon contact with the electrolyte, adjusting the distribution of ion flux from the bulk electrolyte to the anode and the electrons around the anode, thereby affecting the metal nucleation and morphology. An ideal SEI layer should have high electrical resistivity, high ionic conductivity and permeability, strong mechanical stability, and a suitable thickness with a compact structure [24]. Due to the high reactivity of Li/Na metals, the electrolyte undergoes spontaneous decomposition upon contact with their surfaces, forming a non-uniform SEI layer. The SEI film can exhibit variations in thickness and defects, which create highly active sites. Consequently, Li/Na ions tend to deposit preferentially at these sites, leading to the generation of internal stress within the SEI layer. Over time, this stress ruptures the brittle SEI yielding compositional inhomogeneity [64]. During dissolution, the metal dendrites may commence to dissolve from their roots. The remaining part of the protrusions, wrapped by SEI, loses electrical contact with the current collector and cannot participate to ensure the electrochemical reactions, is denoted “dead Li/Na” [65–67]. Hence, new electrolyte formulations, e.g., high-concentration and localized high-concentration electrolytes, are developed to stabilize metal deposition by forming a robust SEI [68]. Additionally, artificial SEI coatings with tailored composition and structure have been extensively studied. There are many published reviews about how the SEI affects metal deposition and interested readers may consult these references [21,34,69,70].

2.2.3. Stress

Stress is another significant external factor that profoundly impacts dendrite growth. Stress can be classified as internal and external stresses. SEIs or interlayers are the primary internal stress. Also, plastic deformation of Li metal due to externally applied pressure can effectively inhibit dendrite growth [71]. The impact of external stress can be explained in two states: steady state and dynamic state [41]. In the steady state, the stress directly determines the mechanical deformation, e.g., interface contacts, which can obstruct dendrite growth and affect significantly the battery performance. In the dynamic state, mechanics, electrochemical reaction, and ion transport have a complex coupling effect on metal deposition during electrochemical cycling. Various computational methods, such as smooth particle hydrodynamics and coarse-grained Monte Carlo methods, have been used to examine the behaviors of metal deposition. Lai et al. conducted large-scale molecular dynamics (MD) simulations with a machine learning potential on Li dendrite growth under external pressure [72]. They found that Li defects and dendrites would gradually fuse and disappear under pressure, indicating that external stress can enhance the ability of metal self-healing (Fig. 2e).

2.2.4. Temperature

Temperature can affect the transport of metal ions and the morphology of nucleation sites [42]. Zhang et al. reported that temperature and atomic diffusion have a coupling effect on the evolution of metal deposition. At high temperatures, the ion diffusion and concentration polarization are accelerated and reduced, respectively, hence effectively inhibiting the vertical growth of dendrites (Figs. 2f and g) [73]. In addition, it has been reported that a high temperature (60 °C) can promote the homogeneous gathering of massive Li ions on the current collector, which then forms large nuclei. As plating continued, these large nuclei gradually expanded and fused, eventually forming a smooth Li [74]. Notably, under high temperatures, the SEI growth rate increases, which may lead to in-plane heterogeneity of the SEI and cause charges to accumulate at the tip, accelerating the growth of dendrites [75]. Hence, temperature has a complex effect on the metal deposition of batteries, which deserves further investigation.

Summary: In recent years, significant efforts have been devoted to unravel the fundamental principles underlying dendrite growth in Li/Na metal batteries. Mathematical models, such as Sand’s time model and space charge theory, have provided valuable tools for predicting dendrite growth. Additionally, initial nucleation behaviors, SEI chemistry, stress, and temperature have been recognized as influential factors that impact dendrite growth. Considering the complexity of metal dendrite growth, advanced characterization techniques and simulation methods are required to deepen the understanding of metal deposition and propagation.

3. Design concept and preparation of vertically heterogeneous structures

In recent years, numerous efforts have been made to avoid the dendrite growth of Li/Na metal batteries [49,76,77]. To-date, three effective methods to inhibit the growth of dendrites have been investigated which include electrolyte formulation, interface optimization, and host design. Homogeneous structures have been proven ineffective in redistributing the ion concentration and the anode electric field in the vertical direction. In contrast, a vertically heterogeneous structure is a viable solution to tailor the ion flux and electric field distribution, thus preventing problematic dendrite growth. Specifically, in conductive-dielectric gradient hosts or interlayers with increasing electrical conductivity from the separator towards the anode, the electric field distribution within the 3D gradient hosts/interlayers is dominated at the bottom area owing to the higher electric conductivity, and this uniform area is wider than that in the fully conductive counterparts, which is verified by electric field simulation [78]. For the lithiophilicity-gradient structures, the distribution of Li ion flux in the gradient scaffold is more concentrated at the bottom, which can be attributed to the higher reactivity and lower overpotential between the lithiophilic seeds and Li ions [79]. In this section, we will give the regulation mechanisms and preparation methods of vertically heterogeneous structures for Li/Na metal batteries.

3.1. Concept of vertically heterogeneous structure

The term “vertically heterogeneous materials” refers to materials with different compositions, structures, and/or physicochemical properties in the vertical direction in a battery component but are identical in the horizontal direction (Fig. 3a). This graded design controls the selective deposition of metals to allow highly stable and long-lifespan rechargeable Li/Na metal batteries. Herein, we will discuss the regulation effects

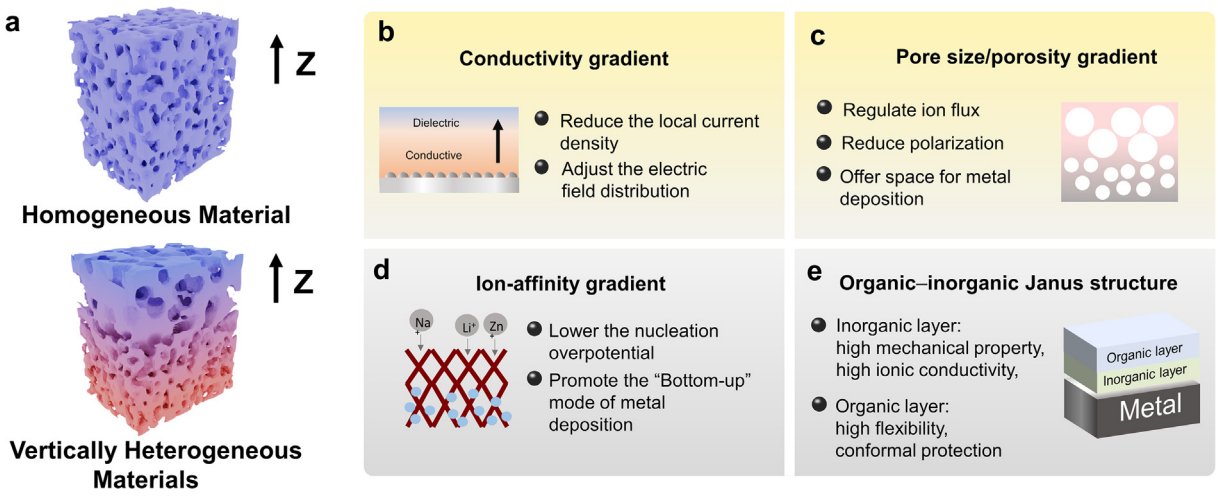

Fig. 3. (a) Schematic showing the concept of vertically heterogeneous material. The Z-axis points to the direction along the anode to the positive. Green, red, and yellow colors represent different structures or components. (b–e) Regulation mechanisms of metal deposition in different heterogeneous structures.

of designing heterogeneous structures to suppress metal dendrite growth, and illustrations are provided in Figs. 3b–e to give a better visualization of different kinds of vertically heterogeneous materials.

3.1.1. *Conductivity gradient framework*

Metal deposition is a diffusion-coupled reaction process, which is mainly determined by multi-physical field parameters such as metal ion concentration, local potentials, and local current [17]. Since the electric and charge-transfer resistances are very similar in electrically conductive and homogeneous hosts, the metal ion transport resistance from the separator to deposition sites governs metal deposition, which is smallest at the anode/separator interface [44,80]. Therefore, metal ions can more easily receive electrons at the anode/separator interface during charging, leading to undesired top growth of metals in conductive hosts and further triggering dendrite formation. To avoid this phenomenon, two kinds of heterogeneous design strategies can be used.

One approach uses the electrical conductivity gradient (Fig. 3b). Based on the conductivity of the host, 3D anodic substrates can be divided into two categories: electrically conductive and dielectric substrates [78]. Conductive substrates enable small polarization and reduce local current density, mitigating dendrite growth [81–83]. Unfortunately, the higher ion concentration and lower transport resistances yield "top growth" of metal on the top of 3D conductive hosts, which not only wastes the internal region of the 3D hosts but stimulates dendrite growth [43]. In contrast, dielectric hosts avoid the top growth of metal associated with their extremely low conductivity (Li ions cannot be reduced at this location) [84,85], but they would lead to large polarization. Conductive-dielectric gradient hosts or interlayers that combine the advantages of both have been recently developed. In essence, the increasing electrical conductivity along the cross-sectional direction would promote the deposition of metals in the conductive region, which harnesses the internal voids of 3D hosts and reduces the potential hazard of piercing the separator by ridding the unwanted top deposition of metal dendrites.

Another approach is ionic conductivity gradient design, which aims to guide the reversible plating/stripping of metal ions into the internal of the host by reducing the local current density on the anode surface. For example, a pore-size gradient framework has been proposed to direct metal deposition (Fig. 3c) [86]. The large pores in the upper layer would reduce the local current density and provide the pathway for the electrolyte to infiltrate into the bottom layer.

3.1.2. *Gradient distribution of ion-affinity sites*

The deposition of metal ions in a battery is governed by the nucleation overpotential, which is the difference between the voltage dip and the plateau [61]. The higher the overpotential, the poorer the ion affinity, and the more difficult the metal nucleates. Significant efforts have been devoted to improving the affinity of the substrate to metal anodes. For Li metal, different kinds of lithiophilic materials have been explored, including metals nanoparticles (Zn, Ag, and Au [87–89]), lithium alloys (Li–Mg, Li–Bi, and Li–Al [90,91]), single atoms (Ni and Pt [92,93]), and metal compounds (MnO and ZnO [94,95]). These materials typically have a high binding energy with Li, and can chemically/electrochemically react with Li, thus acting as lithiophilic sites to lower the nucleation barrier and regulate metal deposition. If the metal affinity sites are by purpose distributed at the bottom region of the substrate to realize an ion affinity gradient, the metal would prefer to deposit at the bottom region of the anode, which has a lower nucleation barrier (Fig. 3d).

3.1.3. *Heterogeneous distribution of stresses in inorganic–organic gradient SEI*

Despite the potential for dendrites to penetrate the separator, the mechanical strength of the root of dendrites is poor. If a high stress is applied to the metal anode, it can have a significant impact on dendrite growth. While SEI can prevent excessive dendrite growth to a certain extent, the fragility of the SEI prevents it from maintaining its integrity for long-term cycling. Much work has been done on the relationship between SEIs and stress [96–98]. For example, Gao et al. proposed the "maximum elastic deformation energy" (U) as an indicator of SEI stability based on Young's modulus and elastic strain limit. A high U allows the SEI to absorb the excess energy generated by anode expansion through elastic deformation, affording much improved electrode stability [99]. During the metal deposition process, the compressive radial stress will decrease monotonically across the SEI layer from the anode/SEI interface to the SEI/electrolyte interface. Meantime, tangential stress that is always tensile and triggers the fracture of SEI, also decreases monotonically across the SEI layer, which has a maximum value at the anode/SEI interface [98,100]. As the tangential stress is much higher than the radial stress, the SEI inner layer is more prone to cracking rather than debonding from the anode surface. Therefore, the use of an inorganic layer with high mechanical strength as the inner SEI is anticipated to prevent lithium dendrite growth and SEI fracture, while an organic-rich layer with high elasticity as the outer SEI can effectively alleviate the SEI deformation, hence enabling stable metal plating/stripping (Fig. 3e).

3.2. *Preparation methods of vertically heterogeneous structures*

As mentioned in Section 3.1, designing vertically heterogeneous structures in anodic hosts, interlayers, artificial SEIs, and electrolytes can

effectively regulate metal deposition. However, the practical fabrication of these heterogeneous structures remains a key issue. In this section, several low-cost and efficient methods to produce heterogeneous structures are summarized, which can be divided into physical and chemical methods.

3.2.1. *Physical methods*

Roll press is a widely accepted approach for fabricating dual-layer anodes due to its low cost and applicability to mass production lines. As a typical example, a lithiophilic–lithiophobic ternary alloy anode was synthesized by rolling Li–Cu alloy foil on Ag foil (Fig. 4a) [101]. The lithiophilic Ag guides the bottom-up growth of Li, leading to stable polarization curves without fluctuations for more than 1200 h in the symmetric cell at a current density of 0.5 mA cm^{-2} and an areal capacity of 0.5 mAh cm^{-2} (Fig. 4b). Surface coating is another convenient method for preparing multilayer structures. Ma et al. presented a Janus face graphene (JFG) substrate for Li metal batteries [102]. Graphene oxide and ammonium chloride (NH_4Cl) were dispersed in deionized water to form a slurry, which was then scraped onto a polyethylene terephthalate (PET) film. After heating under an Ar atmosphere, the as-prepared substrate showed different appearances on two sides (Fig. 4c). The bottom side (JFG1) is dense and rich in nitrogen (N)-doping, while the top side (JFG2) has a porous structure that provides space for Li deposition. As shown in Fig. 4d, the symmetric cell with Li-JFG1 displayed a lower and more steady voltage polarization than Li foil, Li-rGO, and Li-JFG2, demonstrating the ability of a vertically heterogeneous host to direct Li

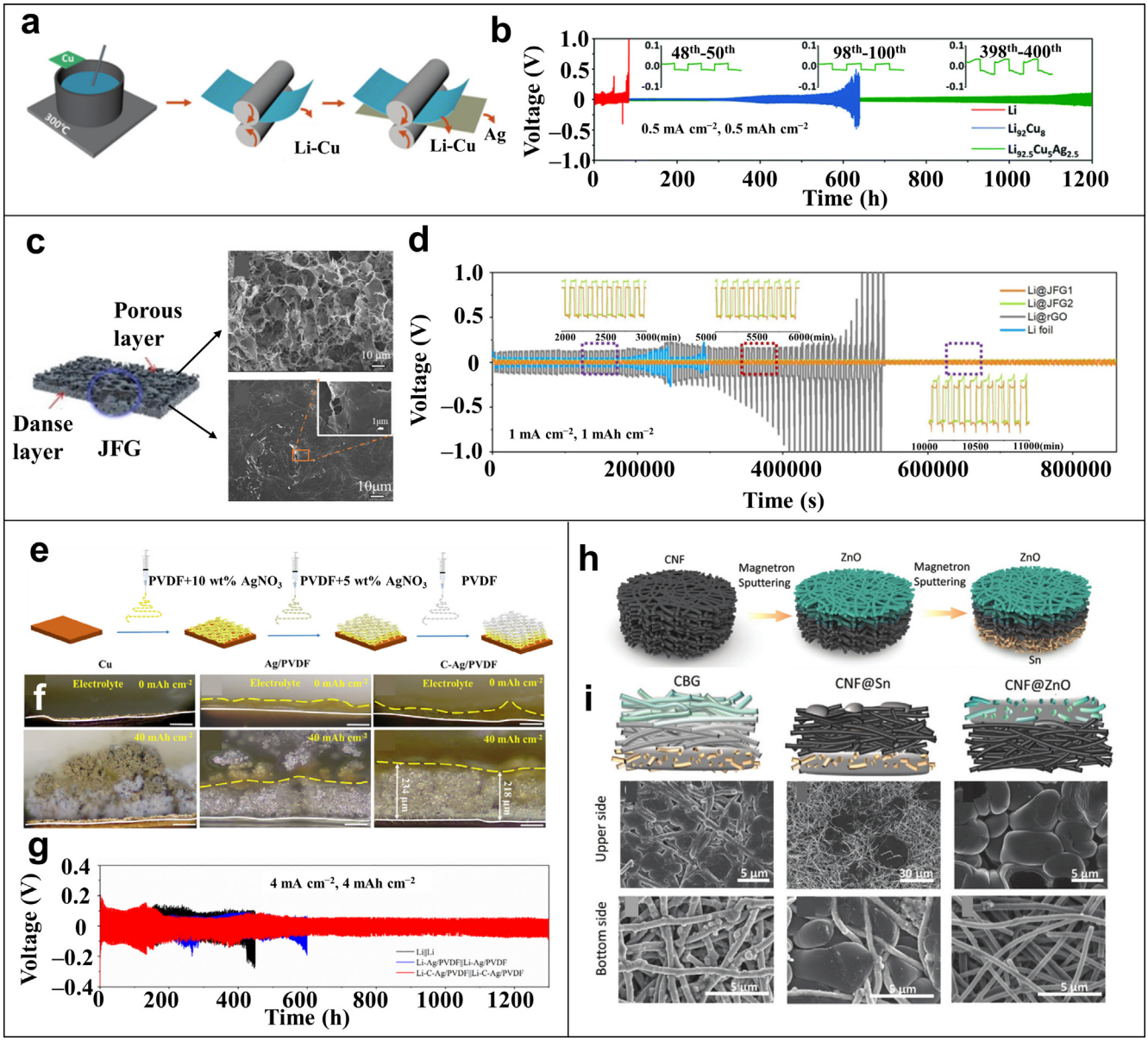

Fig. 4. (a) Schematic illustration of the fabrication process of the Li–Cu–Ag composite anode. (b) Voltage profiles of Li||Li, $Li_{92}Cu_8$||$Li_{92}Cu_8$ and $Li_{92.5}Cu_5Ag_{2.5}$||$Li_{92.5}Cu_5Ag_{2.5}$ symmetric cells with DOL/DME + LiTFSI (3 wt% $LiNO_3$) electrolyte at 0.5 mA cm^{-2}. Reproduced with permission from Ref. [101]. Copyright 2022 The Royal Society of Chemistry. (c) Schematic illustration of the JFG host. (d) Voltage profiles of Li plating/stripping in different symmetric cells at a current density of 1 mA cm^{-2} for 1 h. Reproduced with permission from Ref. [102]. Copyright 2021 Elsevier. (e) Schematic showing the synthetic procedure of the concentration gradient Ag/PVDF (C–Ag/PVDF). (f) *In-situ* optical observations of Li deposition on bare Cu foil, Ag/PVDF, and C–Ag/PVDF at a current density of 5.0 mA cm^{-2}. (g) Polarization curves of Li||Li, Li–Ag/PVDF||Li–Ag/PVDF, and Li–C–Ag/PVDF||Li–C–Ag/PVDF symmetric cells at 4 mA cm^{-2}. Reproduced with permission from Ref. [85]. Copyright 2021 Elsevier. (h) Schematic illustrating the synthesis procedure of CBG (carbon nanofibers with bidirectional gradient modification). (i) Li metal deposition behavior in bare CNF, CNF@ZnO, and CBG hosts. Reproduced with permission from Ref. [108]. Copyright 2016 Wiley-VCH GmbH.

metal deposition and efficiently suppress dendrite growth.

Electrospinning is a well-established approach to synthesize 1D nanostructured materials, which has been successfully applied in the field of batteries [103–106]. Zhao et al. reported a 3D polyvinylidene difluoride (PVDF) framework with an Ag concentration gradient for a Li metal anode by varying the silver nitrate concentration in the electrospinning solution (Fig. 4e) [85]. The porous structure and decorated lithiophilic Ag seeds ensure the "bottom-up" Li growth in the PVDF framework (Fig. 4f). Consequently, Li–C–Ag/PVDF||Li–C–Ag/PVDF symmetric batteries displayed a stable voltage plateau and a long lifespan of > 1200 h at 4 mA cm^{-2} (Fig. 4g). Also, magnetic sputtering has been used to prepare gradient structures for electrospun fiber hosts [107]. An ultralight 3D host with bi-directional lithiophilicity gradient modification was achieved by sputtering [108]. As shown in Fig. 4h, ZnO and Sn nanoparticles were sputtered on the side of CNFs near and away from the separator, respectively. Unlike the homogeneous CNF host, the dielectric ZnO top layer (with an electric resistance of 5.22 kΩ) avoids the reduction of Li ions on the top surface of the host, while the strong affinity of Sn to Li ions promotes selective deposition of Li metal at the bottom region, thus realizing dendrite-free Li deposition inside the host (Fig. 4i).

3.2.2. *Chemical methods*

Chemical methods primarily apply to *in-situ* technology, which can be used in the preparation of batteries. These methods have been widely used in SSE and interface engineering to protect the metal from exposure to air and to ensure the contact of anode and SSE.

Researchers have extensively studied how to improve the stability of SEIs for Li/Na metal batteries. Following this rationale, Guo et al. proposed a dual-layer artificial interface *via* substitution reaction and alloying (Fig. 5a) [109]. The substitution reaction occurred when the Li foil was immersed in silver tetrafluoroborate ($AgBF_4$)/1,2-dimethoxyethane (DME) solution. A top glass layer consisting of LiF and $LiBO_x$ was generated through the reaction of $LiBF_4$ and trace water in the precursor

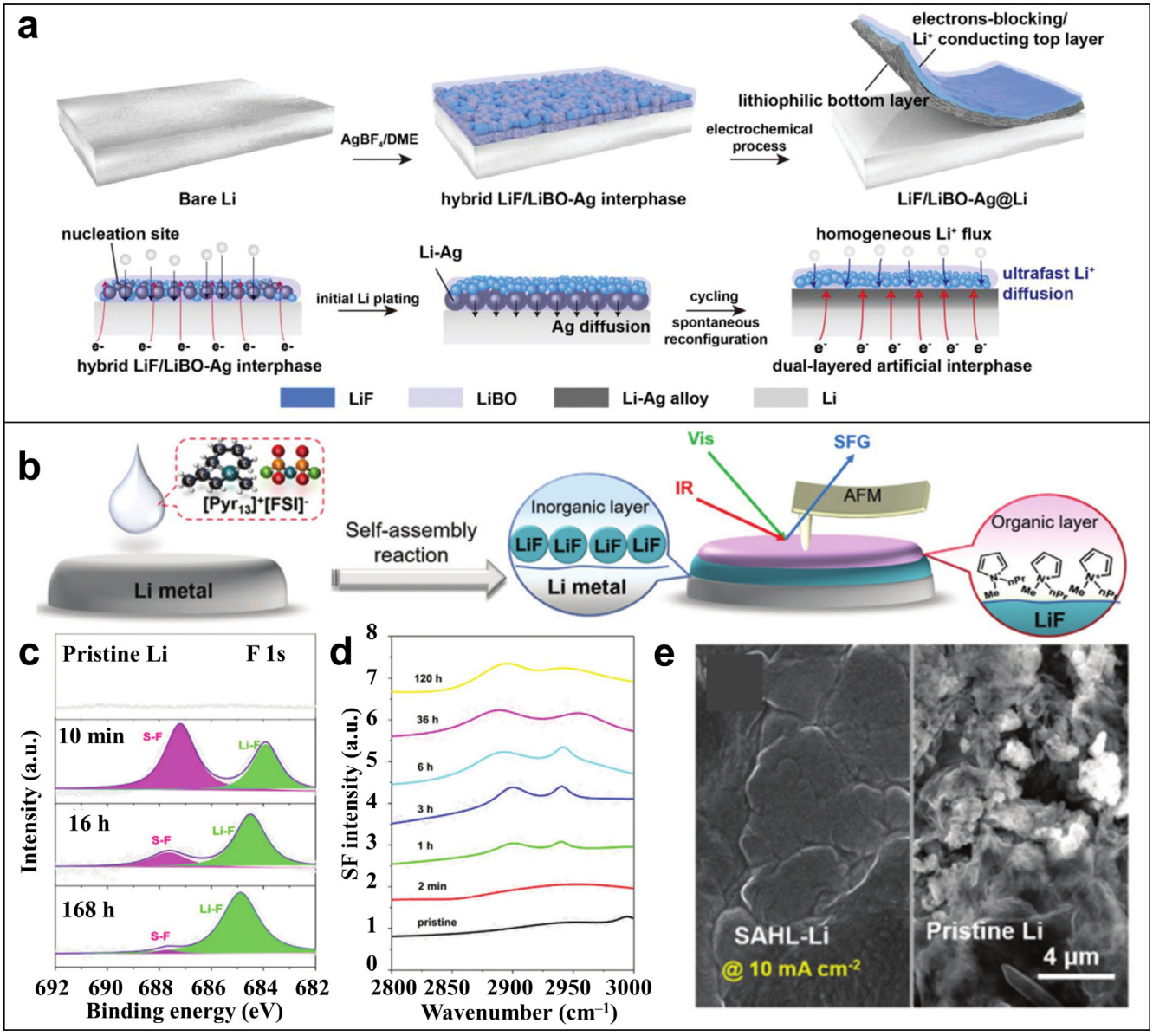

Fig. 5. (a) Schematic showing the spontaneously reconfigured LiF/LiBO–Ag interphase on Li foil. Reproduced with permission from Ref. [109]. Copyright 2023 Wiley-VCH GmbH. (b) Schematic representing the synthesis of ordered SAHL SEI layer on Li metal through self-assembling pretreatment. (c) The high-resolution XPS F1s spectra of the SAHL–Li metal. (d) SFG spectra of Li foil with different time pretreatment. (e) SEM images of the SAHL–Li metal electrode and the pristine Li metal electrode after cycling at 10 mA cm^{-2}. Reproduced with permission from Ref. [110]. Copyright 2020 Wiley-VCH GmbH.

Table 1
Comparison of different manufacturing methods for the preparation of heterogeneous structures.

Methods		Merits	Challenges
Physical methods	Roll press	1) Simple and easy operation 2) Suitable for mass production	1) Li and Na with low mechanical strength and high sticky may break frequently during rolling 2) The operation should be conducted under inert environments
	Coating	1) Cost-effective and easy to operate 2) Suitable for mass production	Difficulty in controlling the horizontal homogeneity of coatings
	Electrospinning	1) Low-cost and high-efficiency 2) Easy assembly into 3D freestanding membranes 3) Controllable sample composition and structure	1) High dependence on environmental conditions 2) Requiring advanced electrospinning techniques to realize mass production.
	Magnetron sputtering	1) Large coating area 2) Highly adhesive and uniform coating layer	1) Requiring high vacuum 2) High prices for some specific targets (e.g., precious metal targets) 3) Long preparation time
Chemical methods	Displacement reactions	1) Simple and easy operation 2) Suitable for mass production	1) Difficulty in precise thickness control 2) Unwanted side reactions
	In-situ polymerization	1) Forming seamless interfaces 2) Avoiding contact with air and moisture	1) Incomplete polymerization may degrade battery performance 2) Unwanted side reactions

solution. This dense and conformal LiF/$LiBO_x$ layer, with a high modulus, effectively suppressed Li dendrites. Finally, Ag was anchored onto the surface of the Li foil, forming a bottom lithiophilic layer caused by the formation of Li–Ag alloy during electrochemical cycling. By the synergistic effect of these two layers, the vertically heterogeneous artificial SEI layer ensures excellent battery performance.

Wang et al. recently presented an organic/inorganic dual-layered interphase using a reactive ionic liquid, i.e., $Pyr_{13}FSI$ [110]. The highly active FSI^- anions react with Li metal to generate a LiF layer, and the organic moieties of RTILs are bound on the Li surface to form the organic layer by ion attraction (Fig. 5b). Further, X-ray photoelectron spectroscopy (XPS) and interface-sensitive sum frequency generation spectroscopy (SFG) confirmed the formation of a gradient interphase at the interface. As shown in Fig. 5c, the peak intensity of LiF increases over time, while the S–F bond in FSI^- anion decreases. The SFG image demonstrated the formation of an organic layer as evidenced by the increased $–CH_2$ (2940 cm^{-1}) and $–CH_3$ (2904 cm^{-1}) Fermi resonance signals (Fig. 5d). The pretreated self-assembled organic/inorganic dual layers on Li metal (SAHL–Li) displayed a smooth and compact surface after electrochemical cycling when compared to severe cracks and dendrites found on the surface of pristine Li (Fig. 5e).

In-situ polymerization is another efficient strategy to prepare heterogeneous structures. Wang et al. developed a separator to produce a gradient-polymerization quasi-solid-state electrolyte [111]. The separator has a tri-layer structure, consisting of a bottom layer of polyethylene (PE) separator, a top layer of lithium hexafluorophosphate ($LiPF_6$), and a middle layer of aluminum oxide (Al_2O_3) to enhance the affinity of the top and bottom layers. The separator is inserted into the cathode and anode with the $LiPF_6$ layer facing the cathode. As $LiPF_6$ is slowly released into the electrolyte, it induces *in-situ* cationic polymerization of 1,3-dioxolane (DOL) upon contact with the ether-based liquid electrolyte, leading to a gradient-polymerization electrolyte with a reducing degree of polymerization from the separator to the cathode. This innovative structure can suppress the shuttle effect and enhance ion transport. The merits/challenges of the physical and chemical methods are summarized in Table 1.

Summary: We have introduced the design concepts of heterogeneous structures, which serve as effective solutions to mitigate uneven metal deposition. These structures effectively address the uneven metal deposition by optimizing the distribution of electric and ionic fields, therefore dissipating internal stresses at the electrolyte-electrode interface, and also enhancing the overall structural stability. Unlike homogeneous structures, the preparation of heterogeneous structures necessitates meticulous arrangement of each component within the structure. While various physical and chemical approaches have been used to construct these structures, the development of scalable and cost-effective production methods remains an ongoing endeavor that demands concerted efforts from both academia and industry.

4. Application of vertically heterogeneous structure for Li/Na metal batteries

In Section 3, a variety of heterogeneous structure designs have been proposed to rectify the uncontrollable metal deposition during plating. These strategies effectively regulate electron and ion transport, enhance structure stability, and dissipate stress, all of which are critical factors in inhibiting dendrite growth. Herein, we overview the application of vertically heterogeneous design in different battery components, including hosts, electrolytes, interlayers, and artificial SEIs.

4.1. Heterogeneous solid electrolytes

The use of conventional liquid electrolytes in batteries has been associated with severe safety hazards due to their flammability and negligible mechanical strength [112]. To overcome these issues, SSEs such as inorganic solid electrolytes (ISEs) and solid polymer electrolytes (SPEs) have been revisited as potential replacements for liquid electrolytes [113]. For example, by adding flame retardants or crosslinkers, it is possible to obtain homogeneous SSE with safety and flexibility [114–116]. However, homogeneous SSEs also have some critical drawbacks that limit their applications in current batteries. Shear modulus, pre-existing defects/cracks, grain boundaries/pores, and electrical conductivity of ISEs cannot completely inhibit metal dendrite growth, and the voids between the ISEs and electrodes cause large cell polarization [117]. SPEs have a narrow electrochemical window that is not suitable for high-voltage cathodes, and their relatively low ion transfer numbers incur a space charge layer [118]. In this context, Ran et al. developed a sandwich composite electrolyte (SCE) with a porous structure to enhance the safety and performance of solid-state batteries [112]. Fig. 6a shows a multilayer SCE prepared by infiltrating PAN and poly(ethylene oxide) (PEO) in a three-layered (porous-dense-porous) SE. The central dense ceramic layer prevents dendrite penetration and offers continuous pathways to improve ion conduction, while the PAN and PEO layers can withstand the redox reaction and achieve seamless contact between electrolyte and electrodes, hence maintaining good structural integrity during cycling due to the polymer softness. The symmetric Na|SCE|Na cell displayed a stable overpotential of ~0.04 V for over 1000 h without short circuits at ambient temperature (Fig. 6b). No PAN peaks are observed in the XRD patterns of PAN-$Na_3Zr_2Si_2PO_{12}$ (NZSP) (Fig. 6c) and all peaks match the pure NZSP electrolyte. Incorporation of ceramic particles can reduce the crystallinity of polymers, which improves the movement of polymer segments and enhances ionic conductivity [119]. Ran et al. solved the poor interfacial contact problem in SSEs by using gradient composite electrolytes (GCEs)

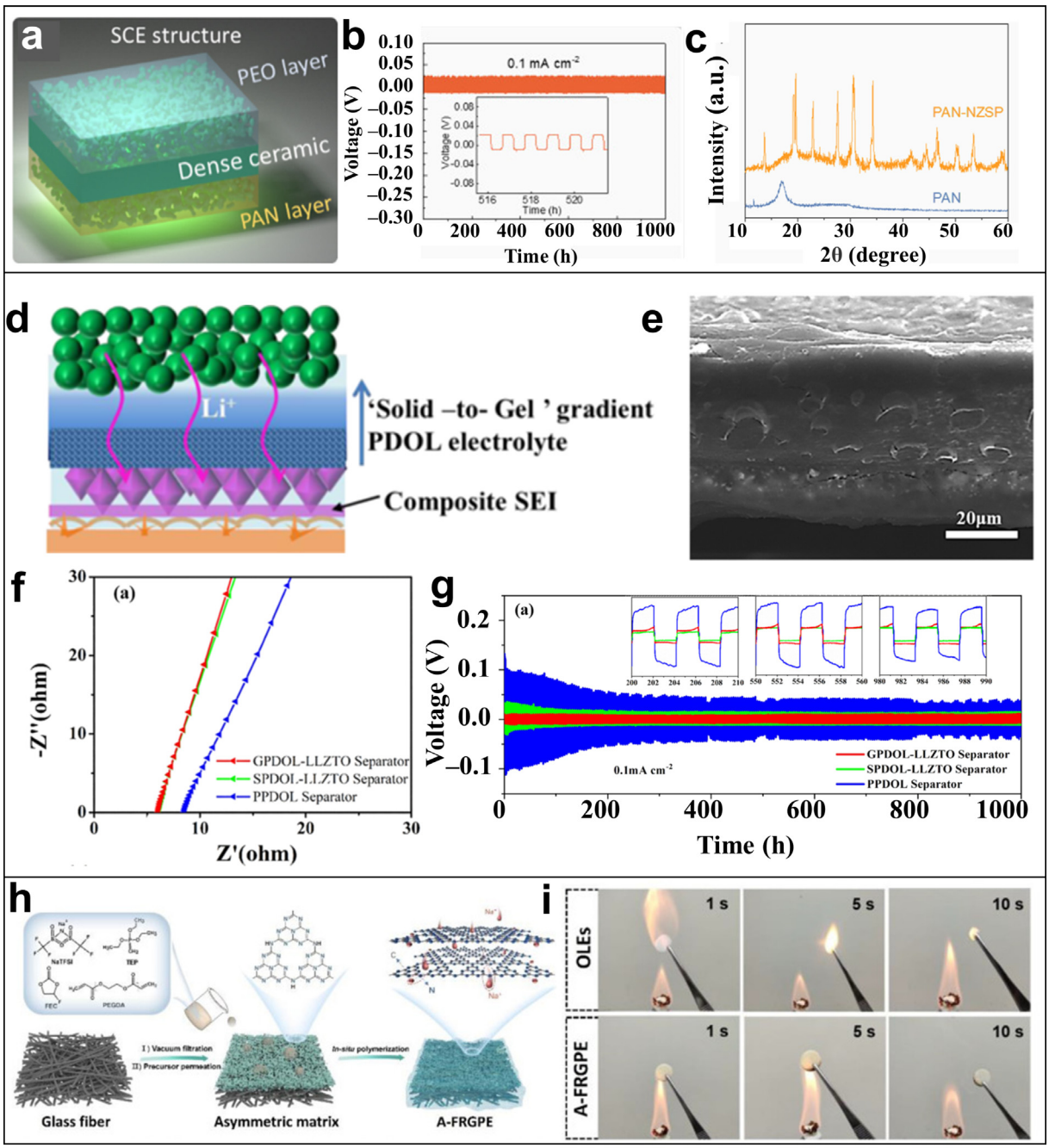

Fig. 6. (a) Schematic illustration of SCE structure. (b) Galvanostatic cycling of Na|SCE|Na symmetric cell at 0.1 mA cm^{-2} with a deposition capacity of 0.1 mAh cm^{-2}. (c) XRD patterns of PAN and NZSP-PAN. Reproduced with permission from Ref. [112]. Copyright 2021 Elsevier. (d) Schematic illustration of SPDOL-LLZTO electrolyte. (e) Cross-sectional SEM image of the separator. (f) Nyquist plots of PPDOL, GPDOL-LLZTO, and SPDOL-LLZTO electrolytes. (g) Voltage-time profiles of symmetric cells using GPDOLR-LLZTO, SPDOL-LLZTO, and PPDOL separators at 0.1 mA cm^{-2}. Reproduced with permission from Ref. [122]. Copyright 2022 American Chemical Society. (h) Schematic showing the fabrication of A-FRGPE. (i) Flammability test of conventional organic liquid electrolyte and A-FRGPE. Reproduced with permission from Ref. [123]. Copyright 2023 Elsevier.

[120]. The Sc, Ge-doped NZSP and PEO were used as ceramic filler and polymer matrix to construct a multilayer GCE. It is known that the growth of dendrite would be inhibited when the electrolyte has a high Young's modulus [121]. Both the conductivity and Young's modulus are markedly increased by increasing NZSP concentration. Hence, the layer with 20 wt% NZSP that has good softness was used to improve the contact of SSE and anode, whereas the middle 40 wt% NZSP-PEO layer enhanced the overall ionic conductivity and inhibited dendrite growth.

Garnet-type $Li_{6.4}La_3Zr_{1.4}Ta_{0.6}O_{12}$ (LLZTO) is another SSE that attracts extensive interest due to its high ionic conductivity and good chemical stability. However, the application of LLZTO electrolytes is hindered by the large interfacial resistance between the anode and electrolyte. Li et al. designed a "solid to gel" gradient structure to improve the compatibility and ion transport at electrode/electrolyte interfaces (Fig. 6d) [122]. A multifunctional composite electrolyte was prepared *via* gradient polymerization and LLZTO coating, denoted as GPDOL-LLZTO. $LiPF_6$ was used as an initiator to trigger the polymerization of DOL and the degree of polymerization can be easily controlled by tuning the amount of $LiPF_6$, thereby forming a gradient structure. Fig. 6e illustrates the cross-sectional scanning electron microscope (SEM) image of the

polymerized composite electrolyte. The electrolyte not only forms a stable SEI film on Li metal to promote uniform ion transportation and inhibit the growth of Li dendrites, but also improves the mechanical property, ionic conductivity, and interfacial compatibility between electrolyte and electrodes. In comparison to PPDOL (a pristine PDOL electrolyte initiated by $LiPF_6$ on PE) and SPDOL-LLZTO separators (an all-solid-state PDOL film prepared by a casting method on the PE skeleton and then coated with an extra LLZTO layer), the GPDOL-LLZTO separator displayed a higher ionic conductivity inferred by the electrochemical impedance spectroscopy (EIS) results (Fig. 6f) and a steadier

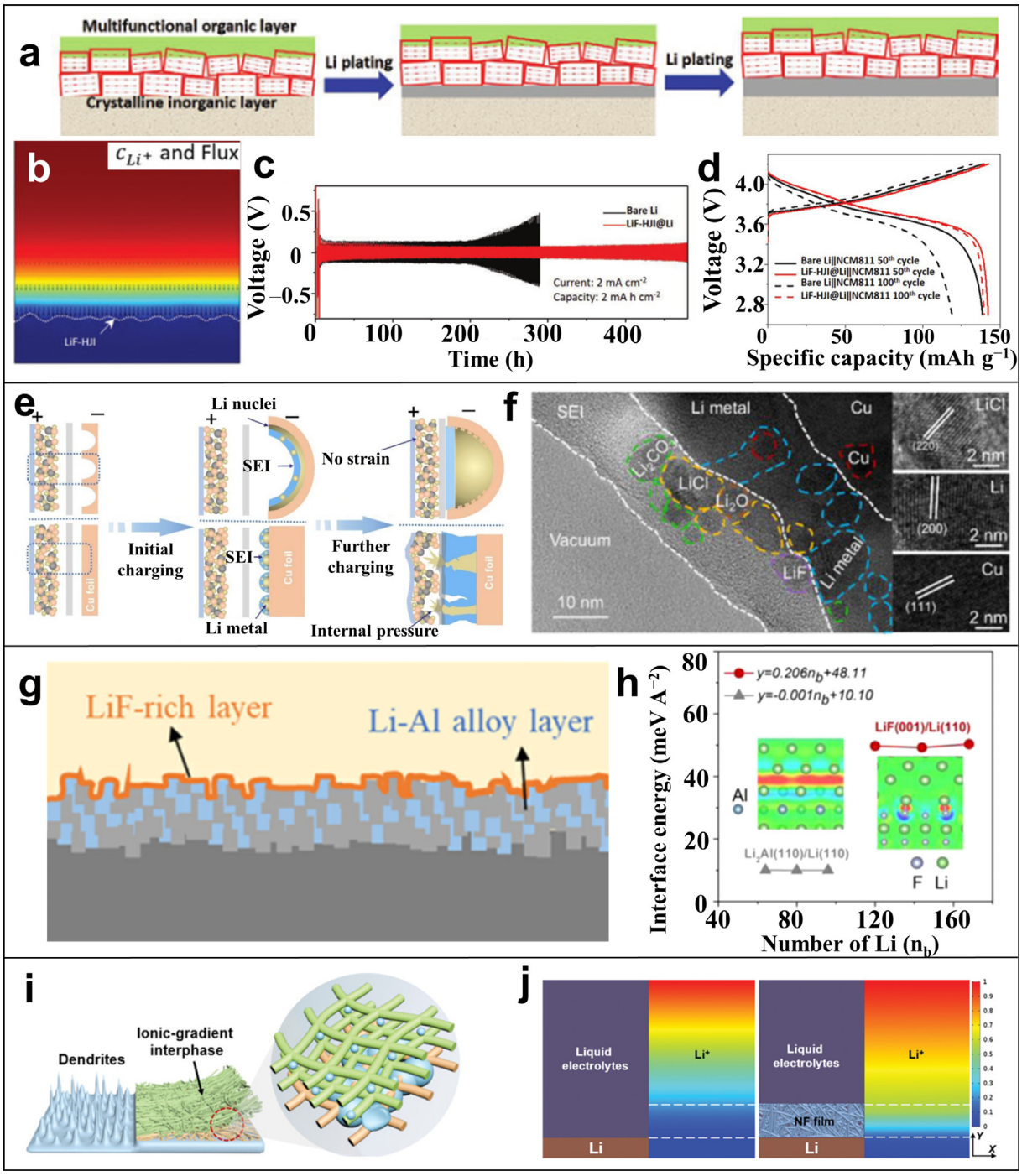

Fig. 7. (a) Schematic illustration of Li plating on ordered multifunctional organic/inorganic hybrid SEI layer. (b) Simulated Li-ion concentration and flux distribution in LiF-HJI@Li. (c) Cycling stability of the symmetric LiF-HJI@Li||LiF-HJI@Li (red) and bare Li||Li (black) cells at a current density of 2 mA cm^{-2} for 1 h. (d) Charge/discharge profiles of full cells with LiF-HJI@Li and bare Li as anodes. Reproduced with permission from Ref. [130]. Copyright 2021 Wiley-VCH GmbH. (e) Schematic illustrations of Li deposition during charging processes on 3D micro-hole-grid (MHG) and two-dimensional (2D) bare Cu foils. (f) HR-TEM image of SEI layer on fully lithiated Cu/copper chloride (CuCl) surface. Reproduced with permission from Ref. [136]. Copyright 2021 Elsevier. (g) Schematic illustration of the morphological evolution of Li/PEO interfaces with Al/Li dual salts. (h) Plots of the relationship between the interface energy for Li_2Al and LiF components and the number of Li metal formula units. Reproduced with permission from Ref. [137]. Copyright 2022 Elsevier. (i) Schematic representation of Li plating on Li metal anodes without and with the ionic gradient lithiophilic interphase protection layer. (j) Simulations of the Li-ion distributions near the Li metal anode without and with the ionic gradient lithiophilic interphase protection layer. Reproduced with permission from Ref. [140]. Copyright 2019 Wiley-VCH GmbH.

overpotential over 1000 h (Fig. 6g). To mitigate the safe issue of sodium–metal batteries (SMBs), Yang et al. recently proposed an asymmetric flame-retardant gel polymer electrolyte (A-FRGPE) for dendrite-free SMBs [123]. To prepare a robust asymmetric glass fiber matrix, a graphitic carbon nitride (g-C_3N_4) layer was coated on a glass fiber by vacuum filtration, and phosphate was encapsulated into the g-C_3N_4 layer as a flame retardant (Fig. 6h). The sodiophilic porous g-C_3N_4 layer near the Na side can regulate uniform Na deposition, effectively suppressing the growth of Na dendrites. At the same time, the introduction of g-C_3N_4 ensures the thermal stability of the battery and improves the flame resistance by coupling with phosphate (Fig. 6i).

4.2. Heterogeneous interfaces

The rupture and regeneration of SEI deplete electrolytes and cause non-uniform ion transport, leading to severe dendrite growth. Uncontrollable dendrite growth further hinders the growth of homogeneous SEI [124]. Therefore, different approaches have been proposed to stabilize the electrode/electrolyte interfaces, which include the creation of artificial SEI and the modification of interlayers/separators [125].

4.2.1. Artificial SEI

In general, SEI forms spontaneously once the highly reactive metal anode contacts with the electrolyte, acting as a protective film and preventing side reactions between the electrode and electrolyte [126]. Engineering an artificial SEI can further protect the anode from continuously reacting with the electrolyte [70,127]. LiF, a critical component in SEI with low electrical conductivity and high electrochemical stability against Li, has been proven helpful for uniform Li deposition [128,129]. Therefore, an ordered LiF-rich and lithiophilic hybrid Janus interphase (LiF-HJI) was developed to stabilize the Li metal anode (Fig. 7a) [130]. The even distribution of inorganic crystalline grains in the inorganic SEI layers is good for uniform Li deposition (Fig. 7b), and the mechanical property of organic layers keeps the interphase from breaking under a large volume change of the anode. As shown in Fig. 7c, the voltage hysteresis of the LiF-HJI@Li anode was lower than that of the bare Li metal anode at a current density of 2 mA cm^{-2} and a deposition capacity of 2 mAh cm^{-2}. Furthermore, the charge/discharge profiles of the full cells with LiF-HJI@Li as anode also showed better stability and smaller polarization (Fig. 7d). Lu et al. focused on Li metal stabilization by developing a polymer–inorganic gradient SEI (PIG-SEI) layer on Li [131]. Poly (ethyleneglycol) diacrylate-co-vinylene carbonate (PEGDA-co-VC), copper fluoride (CuF_2) and lithium nitrate ($LiNO_3$) were co-dissolved in dimethyl ether and dropped onto metallic Li to form a PIG-SEI layer. After *in-situ* curing, the conformal PIG-SEI layer covered the Li metal seamlessly without forming any voids or cracks, which could reduce not only the interfacial resistance of anode/SEI but also inhibited Li dendrite growth. It was observed that nano LiF, lithium nitride (Li_3N), and Cu passivating particles were generated on the metal surface, offering uniformly distributed nucleation sites for Li.

Recently, anode-free metal batteries have received great interest due to their easy fabrication and high energy densities [132–134]. Since there is no active metal in the anode, the Coulombic efficiency (CE) becomes vitally important and is seriously affected by dendrites [135]. Li et al. designed a composite SEI architecture with a gradient lithium chloride (LiCl) concentration on a 3D Cu nanostructure (Fig. 7e) [136]. The inner SEI comprises mainly LiCl, lithium carbonate (Li_2CO_3), and LiF, whereas the outer SEI is rich in polymer (Fig. 7f). Such a dual-layer structure improves Li ion conductivity and mechanical property of SEI, which in turn contribute to smooth Li deposition.

Opposite to liquid electrolytes, SSEs do not easily wet the electrodes spontaneously, resulting in reduced contact area between anode and electrolyte because voids form during metal plating/stripping. Lin et al. introduced a novel SEI, which was prepared by coating a layer containing aluminum trifluoromethanesulfonate ($Al(OTf)_3$) and lithium bis(trifluoromethanesulphonyl) imide (LiTFSI) onto the PEO-based electrolyte (Fig. 7g) [137]. The top lithiophobic LiF-rich layer inhibits dendrite growth caused by its high interface energy against Li and the electron-blocking effect, while the bottom Li–Al alloy layer reduces the interfacial resistance during cycling (Fig. 7h). The full cell paired with $LiFePO_4$ using dual-salt coated PEO electrolyte exhibited impressive cycling performance, which retained 89.1% capacity after 350 cycles at 0.5 C. Encouraged by the outstanding battery performance shown in coin cell configuration, an all-solid-state pouch cell was assembled and tested. The results showed an impressive high capacity of 150.2 mAh g^{-1} (corresponding to 0.60 mAh cm^{-2}) at 0.1 C. Notably, the battery continued to supply power when flipped or cut, demonstrating excellent tolerance to mechanical stress. Xiang et al. proposed a self-formed interphase with a Fe valence gradient to improve the poor anode/electrolyte compatibility and dendrite growth of solid-state SMBs [138]. A sodiophilic α-$Fe_2O_{3-x}F_x$ interlayer was specially coated on NZSP (α-FeOF@NZSP), and in contact with Na, to form a two-layer interphase. The layer near Na containing Fe and NaF could prevent continuous reduction reactions, and the Fe^{2+}/Fe^{3+}-rich layer away from Na served as an anode buffer to store Na metal and avoid uneven deposition of Na. Based on this novel structure, a Na||α-FeOF@NZSP||Na symmetric cell showed outstanding performance for 1000 h under 1 mA cm^{-2} at an elevated temperature of 80 °C. Moreover, the $Na_3V_2(PO_4)_3$ (NVP)|α-FeOF @NZSP|Na full cell exhibited impressive long-term cycling stability over 120 cycles at 1 C and 25 °C, with a high capacity retention of 96%.

4.2.2. Composite interlayers/separators

Although artificial SEI layers can improve the mechanical properties, they may break upon battery cycling. Conventional separators, for example, PE and polypropylene (PP), have been extensively used in different batteries because of their affordability, ease of processing, and excellent electrochemical stability. Nonetheless, these separators have limited electrolyte wettability, which hinders the transport of metal ions and triggers non-uniform deposition of ions on the anode surface [139]. Thus, constructing new interlayers/separators is an alternative method to mitigate metal dendrite growth. Lai et al. synthesized an ionic gradient interface film by electro-spinning to suppress dendrite growth (Fig. 7i) [140]. The nanofiber (NF) layer at the top of the film contains ionic-conductive $Li_{0.33}La_{0.56}TiO_3$ (LLTO), while the bottom region is an NF layer comprising lithiophilic Al_2O_3. This dual-gradient structure enhances the uniform distribution of lithium ions and promotes the bottom-up deposition of Li metal (Fig. 7j). Like CNF film, carbon nanotube (CNT) film is also considered an appropriate carbon-based substrate for Li/Na metal batteries. To fabricate a sodiophobic–sodiophilic interlayer, Ag was decorated on the CNT film with a concentration gradient across the thickness to serve as an interlayer [141]. Na atoms are more likely adsorbed on the Ag-rich side of the interlayer, which can alleviate the growth of Na dendrites and reduce the short circuit risk. Hence, the anode with the sodiophobic-sodiophilic CNT interlayer exhibited ultralong cyclic stability for $>$ 1000 h at a high current density of 8 mA cm^{-2}.

4.3. Heterogeneous hosts

Designing 3D porous anode hosts is a viable strategy to harbor the severe dendrite growth and volume change of Li/Na metal anodes during plating/stripping because of their high surface areas and large internal space [103]. However, metal ions tend to accumulate on the top surface of 3D conductive hosts owing to the higher ion concentration, leading to inefficient use of space within the host and uneven metal deposition. For this reason, heterogeneous designs for anode hosts have been widely studied to promote “bottom-up” growth of Li/Na metal anodes. Recently, different types of vertically heterogeneous structures are proposed to regulate better metal deposition in 3D hosts, for example, pore size and porosity gradient, conductivity gradient, and ion-affinity gradient.

4.3.1. Pore size and porosity gradient

Carbon hosts with numerous pores provide plenty of space for metal deposition, but the impact of pore size on metal deposition is not well understood. Noh et al. accordingly designed a 3D carbon-based porous anode (3D-CPA) with a pore-size gradient to study this issue (Fig. 8a) [142]. The anode was constructed using two different diameters (15 μm and 50 μm) of polymethylmethacrylate (PMMA, a pore-forming agent) mixed with graphite and polyamide-imide (PAI) in N-methyl-2--pyrrolidone (NMP) to form two slurries, which were cast on Cu foil in sequence. After heat-treated for 1 h at 400 °C, PMMA was removed completely and a carbon-based host with large pores in the upper layer and small pores in the bottom layer was obtained. As displayed in the SEM image (Fig. 8b), no Li dendrites were formed on the 3D-CPA surface after depositing 4 mAh cm^{-2} Li at 0.1 mA cm^{-2}, confirming the prominent performance of 3D-CPA to regulate Li deposition. The 3D-CPA also maintained a stable CE for 250 cycles and increased to 97% after the first few cycles.

4.3.2. Conductivity gradient

3D electrically conductive frameworks possess high surface areas and electrical conductivity, which can reduce the local current density and suppress dendrite growth. But the concentrated electric field and ion flux in 3D hosts give rise to the top-growth mode of Li/Na metal anodes. While a dielectric host can prevent the top growth of Li/Na metal anodes, it

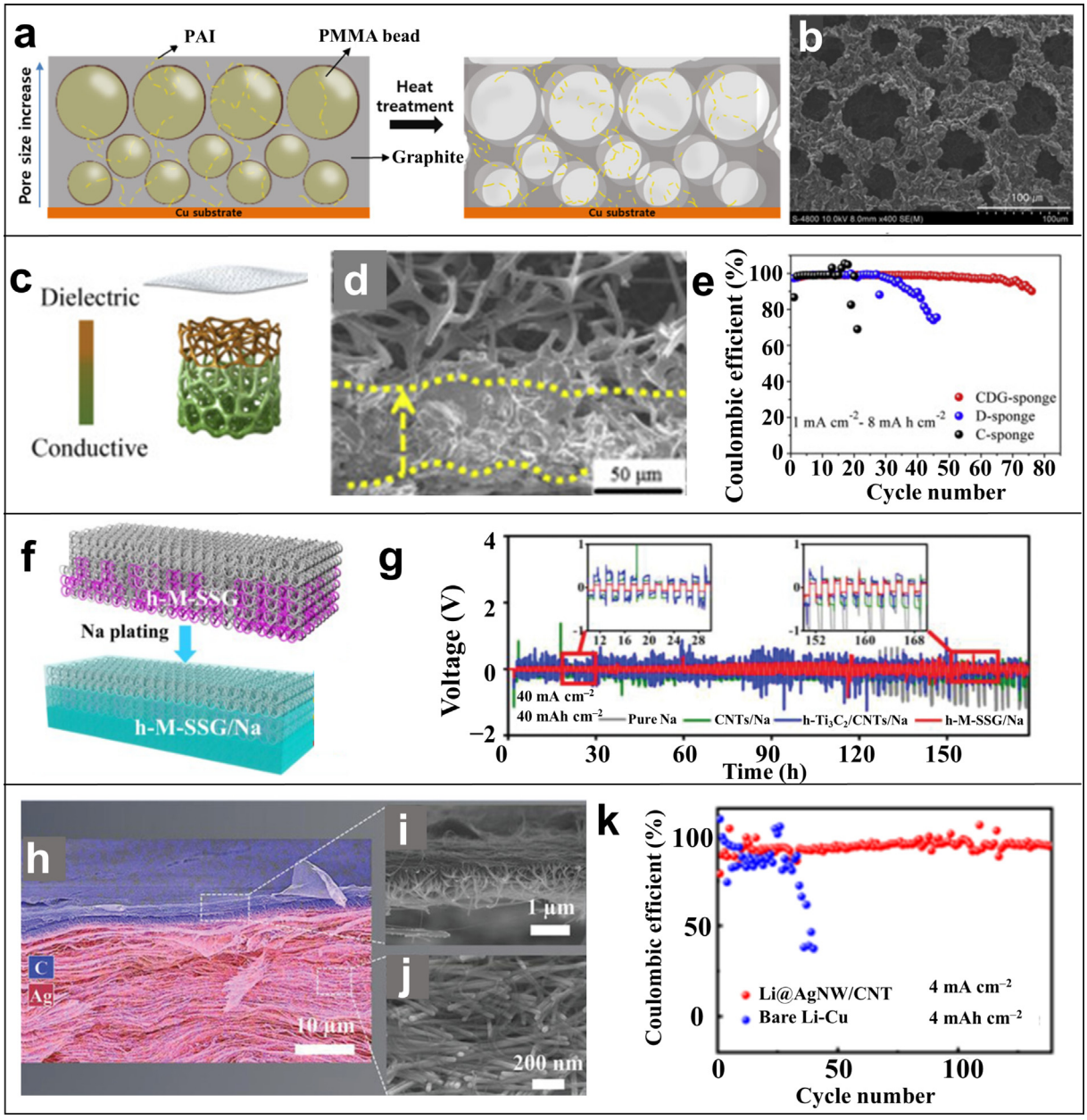

Fig. 8. (a) Schematic representation of 3D-CPA with a pore-size gradient. (b) SEM image showing the top view of 3D-CPA after plating 4 mAh cm^{-2} of Li. Reproduced with permission from Ref. [142]. Copyright 2021 American Chemical Society. (c) Schematic illustration of CDG-sponge. (d) SEM image of CDG-sponge after depositing 5 mAh cm^{-2} at 1 mA cm^{-2}. (e) CE of different sponge-based electrodes cycling at 1 mA cm^{-2} and 8 mAh cm^{-2}. Reproduced with permission from Ref. [78]. Copyright 2019 Elsevier. (f) Schematic illustration of Na deposition on h-M-SSG. (g) Voltage profile of symmetric cells using pure Na, CNTs/Na, h-Ti_3C_2/CNTs/Na, and h-M-SSG/Na electrodes at 40 mA cm^{-2} and 40 mAh cm^{-2}. Reproduced with permission from Ref. [145]. Copyright 2022 Wiley-VCH GmbH. (h) Cross-sectional elemental mapping and (i, j) SEM images of 3D AgNWs/CNT scaffold. (k) The CE of Li@AgNWs/CNT and Li–Cu at 4 mA cm^{-2} and 4 mAh cm^{-2}. Reproduced with permission from Ref. [151]. Copyright 2022 Wiley-VCH GmbH.

increases the battery polarization. In contrast, construction of conductivity gradient hosts combines the advantages of electrically conductive and dielectric hosts to direct metal deposition from the bottom of 3D hosts [143,144]. Li synthesized a conductive-dielectric gradient framework (CDG-sponge) by adding a bottom conductive layer (nickel (Ni) nanolayer) to a top dielectric layer (melamine sponge) (Fig. 8c) [78]. The framework has a gradually changing electrical conductivity in the vertical direction, allowing for "bottom-up" Li metal deposition after depositing 5 mAh cm^{-2} of Li under 1 mA cm^{-2} (Fig. 8d). In comparison with the conductive framework (C-sponge) and dielectric framework (D-sponge), CDG-sponge exhibited better cycling performance, which could operate stably for 65 cycles at a current of 1 mA cm^{-2} and a capacity of 8 mAh cm^{-2}. By sharp contrast, plating/stripping CEs of C-sponge and D-sponge based anodes are dramatically declined after only 20 and 28 cycles, respectively, under the same conditions (Fig. 8e).

4.3.3. Ion-affinity gradient

It has been recognized an effective method to guide the metal deposition by introducing ion-affinity sites [78]. Based on this rationale, He et al. presented a lightweight host with a stepped sodiophilic gradient structure (h-M-SSG) to direct the selective Na metal deposition [145]. The sodiophilic h-Ti_3C_2 content increases from the top to the bottom region of the host, facilitating the bottom-up deposition of Na metal (Fig. 8f). As a result, the h-M-SSG/Na exhibited excellent cycling stability at a high current density of 40 mA cm^{-2} and an areal capacity of 40 mAh cm^{-2} (Fig. 8g). Recently, a low-tortuosity 3D wood-derived carbon (WDC) framework with a graded distribution of lithiophilic sites, such as Ag, ZnO, and Au, was designed [79]. The capillary structure of WDC efficiently promotes Li ions transport to the electroactive areas during plating due to its oriented structure [146]. Meanwhile, the abundant lithiophilic sites at the bottom of the framework promote Li metal deposition.

4.3.4. Multiple gradients

The deposition of metals is driven by multiple factors, e.g., ion concentration, electric field, and wettability. Thus, a single gradient system cannot completely address metal dendrite growth. Hence, the fabrication of anodes with multiple gradients is of great interest [147–150]. A dual-gradient composite anode combining rigidity and flexibility has been designed for Li metal batteries [151]. The anode was synthesized using silver nanowires (AgNWs) as the bottom layer and CNTs as the top layer by a facile filtration method (Figs. 8h–j). The higher conductivity and lithiophilicity of AgNWs than those of CNTs enable a progressive deposition route for metallic Li on the bottom of the battery. Further, the synergistic effect of rigid AgNWs and flexible CNTs helps maintain the electrode integrity during Li plating/stripping. Hence, AgNWs/CNTs hosts maintained high CEs for more than 100 cycles at 4 mA cm^{-2} and a deposition amount of 4 mAh cm^{-2} (Fig. 8k).

Summary: Herein, we provide a comprehensive overview of the applications of vertically heterogeneous structures in Li/Na metal batteries.

Table 2
Heterogeneous structures for Li/Na metal batteries.

	Materials	Battery type	Symmetric cell performance	Full cell	N/P	Ref.
Electrolytes	Sandwich composite electrolyte	Na metal	0.1 mA cm^{-2} and 0.1 mAh cm^{-2} for 1000 h	94 mAh g^{-1} after 460 cycles at 0.2 C with 81% capacity retention	–	[112]
	Gradient composite electrolyte	Na metal	0.2 mA cm^{-2} and 0.2 mAh cm^{-2} for 600 h	84 mAh g^{-1} after 100 cycles at 0.2 C with 88% capacity retention	–	[120]
	Gradient PDOL/LLZTO composite electrolyte	Li metal	0.1 mA cm^{-2} and 0.1 mAh cm^{-2} for 1000 h	120 mAh g^{-1} after 200 cycles at 0.3 C with 82% capacity retention	–	[122]
	Asymmetric flame-retardant gel polymer electrolyte	Na metal	0.1 mA cm^{-2} and 0.1 mAh cm^{-2} for 950 h	119 mAh g^{-1} after 1100 cycles at 1 C with 96.1% capacity retention	–	[123]
Artificial SEIs/ Interlayers	Ordered LiF-rich and lithiophilic hybrid Janus interphase	Li metal	2 mA cm^{-2} and 2 mAh cm^{-2} for 480 h	131.7 mAh g^{-1} after 300 cycles with 80.1% capacity retention	–	[130]
	Polymer-inorganic gradient SEI	Li metal	1 mA cm^{-2} and 2 mAh cm^{-2} for 2500 h	170 mAh g^{-1} after 200 cycles at 0.5 C with 90% capacity retention	–	[131]
	In-situ grown gradient SEI	Li metal	–	100 cycles at 0.5 C with 76.6% capacity retention	–	[136]
	Li/PEO interfaces	Li metal	0.1 mA cm^{-2} for 1000 h	149.2 mAh g^{-1} after 350 cycles at 0.5 C with 89.1% capacity retention	–	[137]
	α-FeOF@NZSP interphase with Fe gradient	Na metal	0.2 mA cm^{-2} for 840 h	95.5 mAh g^{-1} after 120 cycles at 1 C with 96% capacity retention	–	[138]
	Ionic gradient and lithiophilic inter-phase	Li metal	5 mA cm^{-2} and 2.5 mAh cm^{-2} for 1000 h	133.3 mAh g^{-1} after 150 cycles at 5 C with 86% capacity retention	–	[140]
	Sodiophobic–sodiophilic gradient interfacial layer	Na metal	1 mA cm^{-2} and 4 mAh cm^{-2} for 800 h	500 cycles at 2 C with over 99.9% capacity retention	–	[141]
	h-BN@PP@C multifunctional Janus separator	Na metal	3 mA cm^{-2} and 3 mAh cm^{-2} for 1000 h	202.3 mAh g^{-1} after 550 cycles at 500 mA g^{-1} with 71% capacity retention	–	[158]
	Lithiophilic–lithiophobic gradient SEI composed of LiAg–LiF/Li_3N	Li metal	0.2 mA cm^{-2} for over 1100 h	143 mAh g^{-1} after 300 cycles at 0.5 C with 91.4% capacity retention	–	[159]
Anodic hosts	3D-carbon-based porous anode	Li metal	2 mA cm^{-2} and 1.2 mAh cm^{-2} for 680 h	250 cycles at 0.5 C with 99.86% capacity retention	1	[142]
	Conductive-dielectric gradient framework	Li metal	1 mA cm^{-2} and 1 mAh cm^{-2} for 780 h	127.3 mAh g^{-1} after 400 cycles at 1 C with 87.6% capacity retention	–	[78]
	h-Ti_3C_2-based scaffold with stepped sodiophilic gradient structure	Na metal	40 mA cm^{-2} and 40 mAh cm^{-2} for 170 h	–	–	[145]
	3D AgNWs/CNT scaffold	Li metal	30 mA cm^{-2} and 1 mAh cm^{-2} for 500 cycles	–	1	[151]
	Gradient lithiophilic Cu foam	Li metal	1 mA cm^{-2} and 1 mAh cm^{-2} for 450 h	320 cycles at 1 C with 58.74% capacity retention	–	[160]
	Gradiently graphitized carbon framework	Na metal	2 mA cm^{-2} and 4 mAh cm^{-2} for 320 h	73 mAh g^{-1} after 500 cycles at 2.5 C with 99.87% capacity retention	19	[82]

These structures have illustrated effectiveness in mitigating dendrite growth and enhancing battery electrochemical performance. Specifically, we focus on their applications in electrolytes, artificial SEIs/separators, and anodic hosts. Their typical results are summarized in Table 2. It is worth noting that the heterogeneous structure designs have also been extended to other emerging battery systems including zinc (Zn) metal batteries, magnesium (Mg) metal batteries, and aluminum (Al) metal batteries [152–154]. For example, dual-gradient and triple-gradient scaffolds are developed to regulate the selective deposition of Zn metal and Mg metal under harsh conditions, respectively, thereby enhancing the battery's electrochemical performance and safety [155–157]. While heterogeneous structures hold great promise in addressing dendrite-related challenges, it is essential to ensure that other important battery metrics, for example, energy density and production cost, are not significantly affected for practical applications.

5. Conclusion and perspective

The demand for high-energy-density Li/Na metal batteries for transportation, energy storage, and electronic products is increasing rapidly. However, the uncontrollable growth of dendrites remains a significant challenge in the development of Li/Na metal batteries. Dendrites are typically caused by the heterogeneous deposition of metal ions on the anode, and their growth is governed by several factors. Herein, we introduced the growth mechanisms of dendrites, referencing the thermodynamics/kinetics and ion/electron fields, and summarized the various factors that would affect the metal deposition. Then, we proposed the concept of heterogeneous structures and explained how they might inhibit dendrite growth by reconfiguring the physical fields within the cell. We outlined and discussed the current methods for the preparation of heterogeneous structures. Finally, recent developments of heterogeneous structures to control metal deposition were highlighted.

While heterogeneous structures have gained significant attention and are rapidly developing as an important approach to suppress dendrite growth, there remain challenges that must be addressed. The following directions require much further work to advance this field.

(1) Previous studies mainly examined the electrochemical performance of Li/Na metal batteries with vertically heterogeneous-structure designs in coin cells. But, for practical applications, more parameters should be rigorously considered to validate the effectiveness of gradient designs. For example, laboratory testing typically engage higher amounts of electrolyte than commercial cells, and limited electrolyte can lead to concentration polarization even under mild test conditions. The mass ratio of the gradient host should also be minimized without compromising the overall energy density. Thus, lightweight hosts like carbonaceous-based materials are highly desirable. For more realistic results, pouch cells tested under a low N/P ratio (< 3), limited electrolyte amount (< 3 g Ah^{-1}), high current density (> 3 mA cm^{-2}), and areal capacity (3 mAh cm^{-2}) are particularly helpful.

(2) As discussed, a single gradient host or interlayer cannot entirely resolve the dendrite growth issue of Li/Na metal anodes. Hence, tailoring multiple gradients in hosts/interlayers may be a viable solution. Most current fabrication methods, however, require additional processing steps, which consume more time and higher cost. In future work, cost-effective and scalable production methods must be explored. Additive manufacturing strategies, particularly 3D printing techniques, have been widely used recently to fabricate novel battery components with elaborate structures and compositions. 3D printing may be investigated as a suitable method for precisely controlling heterogeneous structures and reducing fabrication costs.

(3) For research on gradient or asymmetric design of solid electrolytes, it is critical to control the thickness to maximize both volumetric and gravimetric energy densities, while reducing the internal resistance. In addition, upscale production methods, e.g., layer-by-layer casting and *in-situ* polymerization, are promising for practical applications. Moreover, additional functions, e.g., thermal shutdown and self-healing, should be embedded to further improve the safety of Li/Na metal batteries.

(4) The understanding of how heterogeneous structures inhibit dendrite growth is limited, and the evolution and retention of gradient structures during operation are mostly overlooked. For instance, *in-situ/operando* optical microscopy has been used to monitor the deposition behavior of metals in gradient hosts [85,148,161]. *In-situ* X-ray tomography and solid-state nuclear magnetic resonance (NMR) techniques offer non-destructive evaluations of metal deposition, while *in-situ* atomic force microscope (AFM) can reveal the mechanical properties of SEIs [99]. Furthermore, examining the retention of gradient structures requires advanced methods such as XPS and SEM. To this end, advanced techniques that are capable of characterizing the structural, chemical and mechanical dynamics with varying temporal and spatial resolutions are highly useful.

(5) As a research tool, computational simulation techniques are essential for the development and application of batteries. Especially, they can also effectively assist the study of dendrite growth in battery systems. Simulation methods, e.g., DFT, MD, and phase field analysis, which are founded on different scales, all have a significant role to help understand how heterogeneous structures govern metal deposition [155,162,163]. However, the application of these simulations in batteries is still immature. For example, some theoretical approaches cannot model the realistic conditions in complex systems containing multi-physical fields. Hence, selecting an appropriate model that matches the gradient battery part is crucial and should be correlated with available experimental datasets. Moreover, advanced modeling with the assistance of artificial intelligence (AI) may provide insights into metal deposition behaviors beyond the reach of experimental data.

Despite the above challenges associated with the applications of heterogeneous structures, experimental results have shown the effectiveness of constructing such structures to guide metal deposition. With continuing research efforts, we believe that various heterogeneous structures will soon be developed and applied to Li/Na metal batteries.

Author contributions

Hongyang Chen: Writing – original draft. **Junxiong Wu:** Writing – review & editing, Writing – original draft, Conceptualization. **Manxian Li:** Writing – review & editing. **Jingyue Zhao:** Writing – review & editing. **Zulin Li:** Writing – review & editing. **Manxi Wang:** Writing – review & editing. **Xuan Li:** Writing – review & editing. **Chuanping Li:** Writing – review & editing. **Xiaochuan Chen:** Writing – review & editing. **Xiaoyan Li:** Writing – review & editing, Conceptualization. **Yiu-Wing Mai:** Writing – review & editing, Conceptualization. **Yuming Chen:** Writing – review & editing, Supervision, Conceptualization.

Declaration of competing interest

The authors declare that they have no known competing financial interests or personal relationships that could have appeared to influence the work reported in this paper.

Acknowledgements

This project was financially supported by the National Natural Science Foundation of China (No. 22209027, No. 22179022, and No. 22109023), the FuXiaQuan National Independent Innovation Demonstration Zone Collaborative Innovation Platform (No. 2022-P-027), the Hundred Talents Plan of Fujian Province, the Top Young Talents of

Young Eagle Program of Fujian Province, the Youth Innovation Fund of Fujian Province (No. 2022J05046 and No. 2021J05043), the Award Program for Fujian Minjiang Scholar Professorship, and the Talent Fund Program of Fujian Normal University.

References

[1] C.Y. Zhao, J. Yan, X.K. Tian, X.J. Xue, Y. Zhao, Progress in thermal energy storage technologies for achieving carbon neutrality, Carbon Neutrality 2 (2023) 10.

[2] Y. Zhao, K.R. Adair, X.L. Sun, Recent developments and insights into the understanding of Na metal anodes for Na-metal batteries, Energy Environ. Sci. 11 (2018) 2673–2695.

[3] L. Ren, B.W. Zhang, Room temperature liquid metals for flexible alkali metal-chalcogen batteries, Exploration 2 (2022) 20210182.

[4] Q.J. Li, W.Y. Wu, Y. Li, H.X. Ren, C. Wu, Y. Bai, Enhanced safety of sulfone-based electrolytes for lithium-ion batteries: broadening electrochemical window and enhancing thermal stability, Energy Mater. Devices 1 (2023) 9370022.

[5] G.M. Zhou, F. Li, H.M. Cheng, Progress in flexible lithium batteries and future prospects, Energy Environ. Sci. 7 (2014) 1307–1338.

[6] L. Ni, G.J. Xu, C.C. Li, G.L. Cui, Electrolyte formulation strategies for potassium-based batteries, Exploration 2 (2022) 20210239.

[7] M.U. Ali, A. Zafar, S.H. Nengroo, S. Hussain, M.J. Alvi, H.-J. Kim, Towards a smarter battery management system for electric vehicle applications: a critical review of lithium-ion battery state of charge estimation, Energies 12 (2019) 446.

[8] Y. Miao, P. Hynan, A. von Jouanne, A. Yokochi, Current Li-ion battery technologies in electric vehicles and opportunities for advancement, Energies 12 (2019) 1074.

[9] Y. Jin, Z.X. Zhao, S. Miao, Q.S. Wang, L. Sun, H.F. Lu, Explosion hazards study of grid-scale lithium-ion battery energy storage station, J. Energy Storage 42 (2021) 102987.

[10] L.Z. Huang, W. Li, Z.M. Cui, Engineering of lithiophilic hosts for stable lithium metal anodes, Energy Mater. 4 (2024) 400030.

[11] J.X. Wu, X.C. Chen, W. Fan, X.Y. Li, Y.-W. Mai, Y.M. Chen, Rationally designed alloy phases for highly reversible alkali metal batteries, Energy Stor. Mater. 48 (2022) 223–243.

[12] R. Zhang, N.-W. Li, X.-B. Cheng, Y.-X. Yin, Q. Zhang, Y.-G. Guo, Advanced micro/nanostructures for lithium metal anodes, Adv. Sci. 4 (2017) 1600445.

[13] H. Liu, Y.C. Ji, Y. Li, S.S. Zheng, Z.H. Dong, K. Yang, A.M. Cao, Y.X. Huang, Y.C. Wang, H.F. Shen, S.-J. Zhang, F. Pan, L.Y. Yang, Regulating lithium affinity of hosts for reversible lithium metal batteries, Interdiscip. Mater. 3 (2024) 297–305.

[14] P. Albertus, S. Babinec, S. Litzelman, A. Newman, Status and challenges in enabling the lithium metal electrode for high-energy and low-cost rechargeable batteries, Nat. Energy 3 (2017) 16–21.

[15] X.Q. Xu, X.B. Cheng, F.N. Jiang, S.J. Yang, D. Ren, P. Shi, H. Hsu, H. Yuan, J.Q. Huang, M. Ouyang, Q. Zhang, Dendrite-accelerated thermal runaway mechanisms of lithium metal pouch batteries, SusMat 2 (2022) 435–444.

[16] Z. Li, J. Huang, B. Yann Liaw, V. Metzler, J.B. Zhang, A review of lithium deposition in lithium-ion and lithium metal secondary batteries, J. Power Sources 254 (2014) 168–182.

[17] Q.Y. Yang, Z. Yu, Y. Li, W. Zhang, H.W. Yuan, H.J. Li, W. Ma, S.M. Zhu, S. Li, Understanding and modifications on lithium deposition in lithium metal batteries, Rare Metal 41 (2022) 2800–2818.

[18] W.W. Han, R.E.A. Ardhi, G.C. Liu, Dual impact of superior SEI and separator wettability to inhibit lithium dendrite growth, Rare Metal 41 (2022) 353–355.

[19] D. Wang, W. Zhang, W.T. Zheng, X.Q. Cui, T. Rojo, Q. Zhang, Towards high-safe lithium metal anodes: suppressing lithium dendrites via tuning surface energy, Adv. Sci. 4 (2017) 1600168.

[20] S.Y. Ni, S.S. Tan, Q.Y. An, L.Q. Mai, Three dimensional porous frameworks for lithium dendrite suppression, J. Energy Chem. 44 (2020) 73–89.

[21] H.P. Wu, H. Jia, C.M. Wang, J.G. Zhang, W. Xu, Recent progress in understanding solid electrolyte interphase on lithium metal anodes, Adv. Energy Mater. 11 (2021) 2003092.

[22] Y.P. Jiang, B. Wang, P. Liu, B. Wang, Y. Zhou, D.L. Wang, H.K. Liu, S.X. Dou, Modified solid-electrolyte interphase toward stable Li metal anode, Nano Energy 77 (2020) 105308.

[23] J. Tan, A. Cannon, E. Ryan, Simulating dendrite growth in lithium batteries under cycling conditions, J. Power Sources 463 (2020) 228187.

[24] D.F. He, J.H. Lu, G.Y. He, H.Q. Chen, Recent advances in solid-electrolyte interphase for Li metal anode, Front. Chem. 10 (2022) 916132.

[25] H.J.S. Sand, On the concentration at the electrodes in a solution, with special reference to the liberation of hydrogen by electrolysis of a mixture of copper sulphate and sulphuric acid, Proc. Phys. Soc. London 17 (1901) 496.

[26] C. Brissot, M. Rosso, J.-N. Chazalviel, S. Lascaud, Dendritic growth mechanisms in lithium/polymer cells, J. Power Sources 81–82 (1999) 925–929.

[27] X.W. Gao, Y.N. Zhou, D.Z. Han, J.Q. Zhou, D.Z. Zhou, W. Tang, J.B. Goodenough, Thermodynamic understanding of Li-dendrite formation, Joule 4 (2020) 1864–1879.

[28] C. Fang, B. Lu, G. Pawar, M. Zhang, D. Cheng, S. Chen, M. Ceja, J.-M. Doux, H. Musrock, M. Cai, B. Liaw, Y.S. Meng, Pressure-tailored lithium deposition and dissolution in lithium metal batteries, Nat. Energy 6 (2021) 987–994.

[29] Y.N. Liu, Z. Xiao, W.K. Zhang, J. Zhang, H. Huang, Y.P. Gan, X.P. He, G.G. Kumar, Y. Xia, Poly(m-phenylene isophthalamide)-reinforced polyethylene oxide composite electrolyte with high mechanical strength and thermostability for all-solid-state lithium metal batteries, Rare Metal 41 (2022) 3762–3773.

[30] J.F. Ding, R. Xu, C. Yan, Y. Xiao, Y.R. Liang, H. Yuan, J.Q. Huang, Integrated lithium metal anode protected by composite solid electrolyte film enables stable quasi-solid-state lithium metal batteries, Chin. Chem. Lett. 31 (2020) 2339–2342.

[31] M.S. Zhang, R.J. Liu, Z.K. Wang, X.Y. Xing, Y.G. Liu, B.B. Deng, T. Yang, Electrolyte additive maintains high performance for dendrite-free lithium metal anode, Chin. Chem. Lett. 31 (2020) 1217–1220.

[32] M.X. Li, H.Y. Chen, Y.X. Wang, X.C. Chen, J.X. Wu, J.Q. Su, M.X. Wang, X. Li, C.P. Li, L.B. Ma, X.Y. Li, Y.M. Chen, Two birds with one stone: engineering siloxane-based electrolytes for high-performance lithium–sulfur polyacrylonitrile batteries, J. Mater. Chem. A 11 (2023) 11721–11729.

[33] C. Li, R. Li, K.N. Liu, R. Si, Z.Z. Zhang, Y.S. Hu, NASICON: a promising solid electrolyte for solid-state sodium batteries, Interdiscip. Mater. 1 (2022) 396–416.

[34] W. Liu, P.C. Liu, D. Mitlin, Review of emerging concepts in SEI analysis and artificial SEI membranes for lithium, sodium, and potassium metal battery anodes, Adv. Energy Mater. 10 (2020) 2002297.

[35] W.W. Li, B. Yang, R.X. Pang, M.Y. Zhang, Sandwiched aramid nanofiber/Al_2O_3-coated polyolefin separators for advanced lithium–sulfur batteries, Compos. Commun. 38 (2023) 101489.

[36] C.X. Chu, R. Li, F.P. Cai, Z.C. Bai, Y.X. Wang, X. Xu, N.N. Wang, J. Yang, S.X. Dou, Recent advanced skeletons in sodium metal anodes, Energy Environ. Sci. 14 (2021) 4318–4340.

[37] G. Wang, C. Song, J.Q. Huang, H.S. Park, Recent advances in carbon-based current collectors/hosts for alkali metal anodes, Energy Environ. Mater. 6 (2023) e12460.

[38] J.N. Wang, Q.Y. Ma, S.Y. Sun, K. Yang, Q. Cai, E. Olsson, X. Chen, Z. Wang, A.M. Abdelkader, Y.S. Li, W. Yan, S.J. Ding, K. Xi, Highly aligned lithiophilic electrospun nanofiber membrane for the multiscale suppression of Li dendrite growth, eScience 2 (2022) 655–665.

[39] D. Han, X. Wang, Y.N. Zhou, J. Zhang, Z. Liu, Z. Xiao, J. Zhou, Z. Wang, J. Zheng, Z. Jia, B. Tian, J. Xie, Z. Liu, W. Tang, A graphene-coated thermal conductive separator to eliminate the dendrite-induced local hotspots for stable lithium cycling, Adv. Energy Mater. 12 (2022) 2201190.

[40] H. Xie, Z. Hao, S. Xie, Y. Ye, W. Zhang, Z. Sun, S. Jin, H. Ji, J. Chen, Molecular sieve based Janus separators for Li-ions redistribution to enable stable lithium deposition, Nano Res. 15 (2022) 5143–5152.

[41] X. Shen, R. Zhang, P. Shi, X. Chen, Q. Zhang, How does external pressure shape Li dendrites in Li metal batteries? Adv. Energy Mater. 11 (2021) 2003416.

[42] J. Wang, W. Huang, A. Pei, Y. Li, F. Shi, X. Yu, Y. Cui, Improving cyclability of Li metal batteries at elevated temperatures and its origin revealed by cryo-electron microscopy, Nat. Energy 4 (2019) 664–670.

[43] S. Zhou, C. Fu, Z. Chang, Y. Zhang, D. Xu, Q. He, S. Chai, X. Meng, M. Feng, Y. Zhang, J. Lin, A. Pan, Conductivity gradient modulator induced highly reversible Li anodes in carbonate electrolytes for high-voltage lithium-metal batteries, Energy Stor. Mater. 47 (2022) 482–490.

[44] J. Wu, Z. Ju, X. Zhang, A.C. Marschilok, K.J. Takeuchi, H. Wang, E.S. Takeuchi, G. Yu, Gradient design for high-energy and high-power batteries, Adv. Mater. 34 (2022) e2202780.

[45] Z. Wang, J. Ni, L. Li, Gradient designs for efficient sodium batteries, ACS Energy Lett. 7 (2022) 4106–4117.

[46] W. Guan, X. Hu, Y. Liu, J. Sun, C. He, Z. Du, J. Bi, K. Wang, W. Ai, Advances in the emerging gradient designs of Li metal hosts, Research 2022 (2022) 9846537.

[47] Z. Li, K. Zhu, P. Liu, L. Jiao, 3D confinement strategy for dendrite-free sodium metal batteries, Adv. Energy Mater. 12 (2021) 2100359.

[48] T.Y. Lyu, F.Q. Luo, D.C. Wang, L.Z. Bu, L. Tao, Z.F. Zheng, Carbon/lithium composite anode for advanced lithium metal batteries: design, progress, in situ characterization, and perspectives, Adv. Energy Mater. 12 (2022) 2201493.

[49] P. Zou, Y. Sui, H. Zhan, C. Wang, H.L. Xin, H.M. Cheng, F. Kang, C. Yang, Polymorph evolution mechanisms and regulation strategies of lithium metal anode under multiphysical fields, Chem. Rev. 121 (2021) 5986–6056.

[50] X.R. Chen, B.C. Zhao, C. Yan, Q. Zhang, Review on Li deposition in working batteries: from nucleation to early growth, Adv. Mater. 33 (2021) e2004128.

[51] J. Chazalviel, Electrochemical aspects of the generation of ramified metallic electrodeposits, Phys. Rev. A 42 (1990) 7355–7367.

[52] C. Monroe, J. Newman, Dendrite growth in lithium/polymer systems, J. Electrochem. Soc. 150 (2003) A1377.

[53] D.R. Ely, R.E. García, Heterogeneous nucleation and growth of lithium electrodeposits on negative electrodes, J. Electrochem. Soc. 160 (2013) A662–A668.

[54] K.N. Wood, E. Kazyak, A.F. Chadwick, K.H. Chen, J.G. Zhang, K. Thornton, N.P. Dasgupta, Dendrites and pits: untangling the complex behavior of lithium metal anodes through operando video microscopy, ACS Cent. Sci. 2 (2016) 790–801.

[55] X.B. Cheng, R. Zhang, C.Z. Zhao, Q. Zhang, Toward safe lithium metal anode in rechargeable batteries: a review, Chem. Rev. 117 (2017) 10403–10473.

[56] F. Wu, Y.-X. Yuan, X.-B. Cheng, Y. Bai, Y. Li, C. Wu, Q. Zhang, Perspectives for restraining harsh lithium dendrite growth: towards robust lithium metal anodes, Energy Stor. Mater. 15 (2018) 148–170.

[57] L. Guo, P.C. Searson, On the influence of the nucleation overpotential on island growth in electrodeposition, Electrochim. Acta 55 (2010) 4086–4091.

[58] A. Mohammadi, L. Monconduit, L. Stievano, R. Younesi, Measuring the nucleation overpotential in lithium metal batteries: never forget the counter electrode, J. Electrochem. Soc. 169 (2022) 070509.

[59] J.-H. Hyun, M.-J. Yi, H. Jung, S.-H. Lee, J.H. Um, S.-H. Yu, Electrochemical behavior and morphological evolution of Li metal anode under high cycling capacity, Energy Stor. Mater. 54 (2023) 146–155.

[60] K. Yan, Z.D. Lu, H.W. Lee, F. Xiong, P.C. Hsu, Y.Z. Li, J. Zhao, S. Chu, Y. Cui, Selective deposition and stable encapsulation of lithium through heterogeneous seeded growth, Nat. Energy 1 (2016) 16010.

[61] X. Guan, A. Wang, S. Liu, G. Li, F. Liang, Y.W. Yang, X. Liu, J. Luo, Controlling nucleation in lithium metal anodes, Small 14 (2018) e1801423.

[62] N. Xu, L. Li, Y. He, Y. Tong, Y. Lu, Understanding the molecular mechanism of lithium deposition for practical high-energy lithium-metal batteries, J. Mater. Chem. A 8 (2020) 6229–6237.

[63] J. Wu, M. Ihsan-Ul-Haq, Y. Chen, J.-K. Kim, Understanding solid electrolyte interphases: advanced characterization techniques and theoretical simulations, Nano Energy 89 (2021) 106489.

[64] X. Shen, R. Zhang, X. Chen, X.B. Cheng, X. Li, Q. Zhang, The failure of solid electrolyte interphase on Li metal anode: structural uniformity or mechanical strength? Adv. Energy Mater. 10 (2020) 1903645.

[65] C. Jin, T. Liu, O. Sheng, M. Li, T. Liu, Y. Yuan, J. Nai, Z. Ju, W. Zhang, Y. Liu, Y. Wang, Z. Lin, J. Lu, X. Tao, Rejuvenating dead lithium supply in lithium metal anodes by iodine redox, Nat. Energy 6 (2021) 378–387.

[66] X.-R. Chen, C. Yan, J.-F. Ding, H.-J. Peng, Q. Zhang, New insights into "dead lithium" during stripping in lithium metal batteries, J. Energy Chem. 62 (2021) 289–294.

[67] M. Werres, Y. Xu, H. Jia, C. Wang, W. Xu, A. Latz, B. Horstmann, Origin of heterogeneous stripping of lithium in liquid electrolytes, ACS Nano 17 (2023) 10218–10228.

[68] X. Li, Y. Pan, Y. Liu, Y. Jie, S. Chen, S. Wang, Z. He, X. Ren, T. Cheng, R. Cao, S. Jiao, Understanding steric hindrance effect of solvent molecule in localized high-concentration electrolyte for lithium metal batteries, Carbon Neutrality 2 (2023) 34.

[69] J. Tan, J. Matz, P. Dong, J. Shen, M. Ye, A growing appreciation for the role of LiF in the solid electrolyte interphase, Adv. Energy Mater. 11 (2021) 2100046.

[70] P. Zhai, L. Liu, X. Gu, T. Wang, Y. Gong, Interface engineering for lithium metal anodes in liquid electrolyte, Adv. Energy Mater. 10 (2020) 2001257.

[71] P. Barai, K. Higa, V. Srinivasan, Impact of external pressure and electrolyte transport properties on lithium dendrite growth, J. Electrochem. Soc. 165 (2018) A2654–A2666.

[72] G. Lai, Y. Zuo, J. Jiao, C. Fang, Q. Liu, F. Zhang, Y. Jiang, L. Sheng, B. Xu, C. Ouyang, J. Zheng, The mechanism of external pressure suppressing dendrites growth in Li metal batteries, J. Energy Chem. 79 (2023) 489–494.

[73] Y. Zhang, Y. Li, W. Shen, K. Li, Y. Lin, Important role of atom diffusion in dendrite growth and the thermal self-healing mechanism, ACS Appl. Energy Mater. 6 (2023) 1933–1945.

[74] K. Yan, J. Wang, S. Zhao, D. Zhou, B. Sun, Y. Cui, G. Wang, Temperature-dependent nucleation and growth of dendrite-free lithium metal anodes, Angew. Chem. Int. Ed. 58 (2019) 11364–11368.

[75] X. Cao, Y. Lu, X. Song, Z. Yuan, F. Wang, Perspective of unstable solid electrolyte interphase induced lithium dendrite growth: role of thermal effect, Electrochim. Acta 439 (2023) 141722.

[76] D. Li, B. Chen, H. Hu, W.Y. Lai, Constructing 3D porous current collectors for stable and dendrite-free lithium metal anodes, Adv. Sustain. Syst. 6 (2022) 2200010.

[77] K. Subramanian, G.V. Alexander, K. Karthik, S. Patra, M.S. Indu, O.V. Sreejith, R. Viswanathan, J. Narayanasamy, R. Murugan, A brief review of recent advances in garnet structured solid electrolyte based lithium metal batteries, J. Energy Storage 33 (2021) 102157.

[78] J. Li, P. Zou, S.W. Chiang, W. Yao, Y. Wang, P. Liu, C. Liang, F. Kang, C. Yang, A conductive-dielectric gradient framework for stable lithium metal anode, Energy Stor. Mater. 24 (2020) 700–706.

[79] Z. Zhu, B. Liu, Y. Qian, Y. Fang, X. Lei, X. Liu, J. Zhou, Y. Qian, G. Wang, Spatially distributed lithiophilic gradient in low-tortuosity 3D hosts via capillary action for high-performance Li metal anodes, Adv. Energy Mater. 13 (2022) 2203687.

[80] J. Pu, J. Li, K. Zhang, T. Zhang, C. Li, H. Ma, J. Zhu, P.V. Braun, J. Lu, H. Zhang, Conductivity and lithiophilicity gradients guide lithium deposition to mitigate short circuits, Nat. Commun. 10 (2019) 1896.

[81] Y. Nan, S. Li, Y. Shi, S. Yang, B. Li, Gradient-distributed nucleation seeds on conductive host for a dendrite-free and high-rate lithium metal anode, Small 15 (2019) e1903520.

[82] Z. Sun, Y. Ye, J. Zhu, E. Zhou, J. Xu, M. Liu, X. Kong, S. Jin, H. Ji, Regulating sodium deposition through gradiently-graphitized framework for dendrite-free Na metal anode, Small 18 (2022) e2107199.

[83] X. Zheng, W. Yang, Z. Wang, L. Huang, S. Geng, J. Wen, W. Luo, Y. Huang, Embedding a percolated dual-conductive skeleton with high sodiophilicity toward stable sodium metal anodes, Nano Energy 69 (2020) 104387.

[84] Q. Ran, L. Wang, L. Li, Y. Zhao, Z. Lu, S. Chen, J. Zou, P. Chen, J. Gao, X. Niu, 3D oxidized polyacrylonitrile/Ag framework guided bottom-up lithium deposition for dendrite-free lithium metal batteries, Chem. Eng. J. 426 (2021) 130780.

[85] Y. Zhao, L. Wang, J. Zou, Q. Ran, L. Li, P. Chen, H. Yu, J. Gao, X. Niu, Bottom-up lithium growth guided by Ag concentration gradient in 3D PVDF framework towards stable lithium metal anode, J. Energy Chem. 65 (2022) 666–673.

[86] J. Lee, E.S. Won, D.M. Kim, H. Kim, B. Kwon, K. Park, S. Jo, S. Lee, J.W. Lee, K.T. Lee, Three-dimensional porous frameworks for Li metal batteries: superconformal versus conformal Li growth, ACS Appl. Mater. Interfaces 13 (2021) 33056–33065.

[87] S.S. Chi, Q. Wang, B. Han, C. Luo, Y. Jiang, J. Wang, C. Wang, Y. Yu, Y. Deng, Lithiophilic Zn sites in porous CuZn alloy induced uniform Li nucleation and dendrite-free Li metal deposition, Nano Lett. 20 (2020) 2724–2732.

[88] B. Tian, Z. Huang, X. Xu, X. Cao, H. Wang, T. Xu, D. Kong, Z. Zhang, J. Xu, J. Zang, X. Li, Y. Wang, Three-dimensional Ag/carbon nanotube-graphene foam for high performance dendrite free lithium/sodium metal anodes, J. Mater. Sci. Technol. 132 (2023) 50–58.

[89] W. Wu, D. Ning, J. Zhang, G. Liu, L. Zeng, H. Yao, M. Wang, L. Deng, L. Yao, Ultralight lithiophilic three-dimensional lithium host for stable high-energy-density anode-free lithium metal batteries, Energy Stor. Mater. 63 (2023) 102974.

[90] T. Krauskopf, B. Mogwitz, C. Rosenbach, W.G. Zeier, J. Janek, Diffusion limitation of lithium metal and Li–Mg alloy anodes on LLZO type solid electrolytes as a function of temperature and pressure, Adv. Energy Mater. 9 (2019) 1902568.

[91] D. He, W. Cui, X. Liao, X. Xie, M. Mao, X. Sang, P. Zhai, Y. Zhao, Y. Huang, W. Zhao, Electronic localization derived excellent stability of Li metal anode with ultrathin alloy, Adv. Sci. 9 (2022) e2105656.

[92] S. Zhang, X. Ao, J. Huang, B. Wei, Y. Zhai, D. Zhai, W. Deng, C. Su, D. Wang, Y. Li, Isolated single-atom Ni–N_5 catalytic site in hollow porous carbon capsules for efficient lithium–sulfur batteries, Nano Lett. 21 (2021) 9691–9698.

[93] W. Zhao, J. Wang, R. Yin, B. Li, X. Huang, L. Zhao, L. Qian, Single-atom Pt supported on holey ultrathin g-C_3N_4 nanosheets as efficient catalyst for Li-O_2 batteries, J. Colloid Interface Sci. 564 (2020) 28–36.

[94] Y. Liu, J. Sun, X. Hu, Y. Li, H. Du, K. Wang, Z. Du, X. Gong, W. Ai, W. Huang, Lithiophilic sites dependency of lithium deposition in Li metal host anodes, Nano Energy 94 (2022) 106883A.

[95] X. Chen, Z. Yuan, J. He, L. Tong, Y. Wang, J. Wu, X. Li, Y. Chen, A lithiophilic MnO@biomass-derived carbon nanofiber host for stable lithium-metal batteries, Compos. Commun. 42 (2023) 101660.

[96] J. Zheng, H. Zheng, R. Wang, L. Ben, W. Lu, L. Chen, L. Chen, H. Li, 3D visualization of inhomogeneous multi-layered structure and Young's modulus of the solid electrolyte interphase (SEI) on silicon anodes for lithium ion batteries, Phys. Chem. Chem. Phys. 16 (2014) 13229–13238.

[97] Q. Tu, L. Barroso-Luque, T. Shi, G. Ceder, Electrodeposition and mechanical stability at lithium-solid electrolyte interface during plating in solid-state batteries, Cell Rep. Phys. Sci. 1 (2020) 100106.

[98] Y. Ali, N. Iqbal, I. Shah, S. Lee, Mechanical stability of the heterogenous bilayer solid electrolyte interphase in the electrodes of lithium–ion batteries, Mathematics 11 (2023) 543.

[99] Y. Gao, X. Du, Z. Hou, X. Shen, Y.-W. Mai, J.-M. Tarascon, B. Zhang, Unraveling the mechanical origin of stable solid electrolyte interphase, Joule 5 (2021) 1860–1872.

[100] Y. He, H. Hu, K. Zhang, S. Li, J. Chen, Mechanical insights into the stability of heterogeneous solid electrolyte interphase on an electrode particle, J. Mater. Sci. 52 (2016) 2836–2848.

[101] Y. Liu, Q. Li, Q. Yao, X. Zhou, W. Wang, K. Chen, Q. Zhu, G. He, A lithiophilic/lithiophobic ternary alloy anode with Ag concentration gradients guides uniform Li deposition, Chem. Commun. 58 (2022) 3158–3161.

[102] J. Ma, J. Yang, Y. Zhao, Q. Ma, Z. Wang, W. Qian, B. Xia, L. Li, W. Zeng, J. Chen, H. Xu, S. Chen, D. He, Z. Wang, S. Mu, Janus-faced graphene substrate stabilizes lithium metal anode, Chem. Eng. J. 433 (2022) 133561.

[103] H. Chen, M. Li, C. Li, X. Li, Y. Wu, X. Chen, J. Wu, X. Li, Y. Chen, Electrospun carbon nanofibers for lithium metal anodes: progress and perspectives, Chin. Chem. Lett. 33 (2022) 141–152.

[104] X. Liu, Y. Zhang, X. Guo, H. Pang, Electrospun metal–organic framework nanofiber membranes for energy storage and environmental protection, Adv. Fiber Mater. 4 (2022) 1463–1485.

[105] F. Shi, C. Chen, Z.L. Xu, Recent advances on electrospun nanofiber materials for post–lithium ion batteries, Adv. Fiber Mater. 3 (2021) 275–301.

[106] M. Wang, S. Lv, M. Li, X. Li, C. Li, Z. Li, X. Chen, J. Wu, X. Li, Y. Chen, Q. Chen, A heterogeneous quasi-solid-state hybrid electrolyte constructed from electrospun nanofibers enables robust electrode/electrolyte interfaces for stable lithium metal batteries, Adv. Fiber Mater. 6 (2024) 727–738.

[107] J. Wu, P. Zou, M. Ihsan-Ul-Haq, N. Mubarak, A. Susca, B. Li, F. Ciucci, J.K. Kim, Sodiophilically graded gold coating on carbon skeletons for highly stable sodium metal anodes, Small 16 (2020) e2003815.

[108] T. Li, S. Gu, L. Chen, L. Zhang, X. Qin, Z. Huang, Y.B. He, W. Lv, F. Kang, Bidirectional lithiophilic gradients modification of ultralight 3D carbon nanofiber host for stable lithium metal anode, Small 18 (2022) e2203273.

[109] J.C. Guo, S.J. Tan, C.H. Zhang, W.P. Wang, Y. Zhao, F. Wang, X.S. Zhang, R. Wen, Y. Zhang, M. Fan, S. Xin, J. Zhang, Y.G. Guo, A self-reconfigured, dual-layered artificial interphase toward high-current-density quasi-solid-state lithium metal batteries, Adv. Mater. 35 (2023) e2300350.

[110] J. Wang, J. Yang, Q. Xiao, J. Zhang, T. Li, L. Jia, Z. Wang, S. Cheng, L. Li, M. Liu, H. Liu, H. Lin, Y. Zhang, In situ self-assembly of ordered organic/inorganic dual-layered interphase for achieving long-life dendrite-free Li metal anodes in LiFSI-based electrolyte, Adv. Funct. Mater. 31 (2020) 2007434.

[111] W.P. Wang, J. Zhang, Y.X. Yin, H. Duan, J. Chou, S.Y. Li, M. Yan, S. Xin, Y.G. Guo, A rational reconfiguration of electrolyte for high-energy and long-life lithium-chalcogen batteries, Adv. Mater. 32 (2020) e2000302.

[112] L. Ran, M. Li, E. Cooper, B. Luo, I. Gentle, L. Wang, R. Knibbe, Enhanced safety and performance of high-voltage solid-state sodium battery through trilayer, multifunctional electrolyte design, Energy Stor. Mater. 41 (2021) 8–13.

[113] L. Wu, Y. Wang, X. Guo, P. Ding, Z. Lin, H. Yu, Interface science in polymer-based composite solid electrolytes in lithium metal batteries, SusMat 2 (2022) 264–292.

[114] C.C. Sun, A. Yusuf, S.W. Li, X.L. Qi, Y. Ma, D.Y. Wang, Metal organic frameworks enabled rational design of multifunctional PEO-based solid polymer electrolytes, Chem. Eng. J. 414 (2021) 128702.
[115] B. Zhou, M. Yang, C. Zuo, G. Chen, D. He, X. Zhou, C. Liu, X. Xie, Z. Xue, Flexible, self-healing, and fire-resistant polymer electrolytes fabricated via photopolymerization for all-solid-state lithium metal batteries, ACS Macro Lett. 9 (2020) 525–532.
[116] M. Yang, F. Feng, Y. Ren, S. Chen, F. Chen, D. Chu, J. Guo, Z. Shi, T. Cai, W. Zhang, Z.F. Ma, S. Chen, T. Liu, Coupling anion-capturer with polymer chains in fireproof gel polymer electrolyte enables dendrite-free sodium metal batteries, Adv. Funct. Mater. 33 (2023) 2305383.
[117] X. Ke, Y. Wang, L. Dai, C. Yuan, Cell failures of all-solid-state lithium metal batteries with inorganic solid electrolytes: lithium dendrites, Energy Stor. Mater. 33 (2020) 309–328.
[118] N. Meng, F. Lian, G. Cui, Macromolecular design of lithium conductive polymer as electrolyte for solid-state lithium batteries, Small 17 (2021) e2005762.
[119] H. Duan, M. Fan, W.P. Chen, J.Y. Li, P.F. Wang, W.P. Wang, J.L. Shi, Y.X. Yin, L.J. Wan, Y.G. Guo, Extended electrochemical window of solid electrolytes via heterogeneous multilayered structure for high-voltage lithium metal batteries, Adv. Mater. 31 (2019) e1807789.
[120] L. Ran, S. Tao, I. Gentle, B. Luo, M. Li, M. Rana, L. Wang, R. Knibbe, Stable interfaces in a sodium metal-free, solid-state sodium–ion battery with gradient composite electrolyte, ACS Appl. Mater. Interfaces 13 (2021) 39355–39362.
[121] M.D. Tikekar, S. Choudhury, Z. Tu, L.A. Archer, Design principles for electrolytes and interfaces for stable lithium–metal batteries, Nat. Energy 1 (2016) 16114.
[122] L.X. Li, R. Li, Z.H. Huang, H. Yang, M.Q. Liu, J. Xiang, S. Hussain, X.Q. Shen, M.X. Jing, A multifunctional gradient solid electrolyte remarkably improving interface compatibility and ion transport in solid-state lithium battery, ACS Appl. Mater. Interfaces 14 (2022) 30786–30795.
[123] M. Yang, F. Feng, Z. Shi, J. Guo, R. Wang, Z. Xu, Z. Liu, T. Cai, Z. Wang, C. Wang, S. Chen, Z.F. Ma, T. Liu, Facile design of asymmetric flame-retardant gel polymer electrolyte with excellent interfacial stability for sodium metal batteries, Energy Stor. Mater. 56 (2023) 611–620.
[124] J.H. Tian, T. Jiang, M. Wang, Z. Hu, X. Zhu, L. Zhang, T. Qian, C. Yan, In situ/operando spectroscopic characterizations guide the compositional and structural design of lithium–sulfur batteries, Small Methods 4 (2019) 1900467.
[125] J. Wang, L. Li, H. Hu, H. Hu, Q. Guan, M. Huang, L. Jia, H. Adenusi, K.V. Tian, J. Zhang, S. Passerini, H. Lin, Toward dendrite-free metallic lithium anodes: from structural design to optimal electrochemical diffusion kinetics, ACS Nano 16 (2022) 17729–17760.
[126] W. Xu, X. Liao, W. Xu, C. Sun, K. Zhao, Y. Zhao, C. Hu, Gradient SEI layer induced by liquid alloy electrolyte additive for high rate lithium metal battery, Nano Energy 88 (2021) 106237.
[127] B. Wu, C. Chen, D.L. Danilov, Z. Chen, M. Jiang, R.A. Eichel, P.H.L. Notten, Dual additives for stabilizing Li deposition and SEI formation in anode-free Li–metal batteries, Energy Environ. Mater. 7 (2023) e12642.
[128] D. Lin, Y. Liu, W. Chen, G. Zhou, K. Liu, B. Dunn, Y. Cui, Conformal lithium fluoride protection layer on three-dimensional lithium by nonhazardous gaseous reagent freon, Nano Lett. 17 (2017) 3731–3737.
[129] W. Huang, H. Wang, D.T. Boyle, Y. Li, Y. Cui, Resolving nanoscopic and mesoscopic heterogeneity of fluorinated species in battery solid-electrolyte interphases by cryogenic electron microscopy, ACS Energy Lett. 5 (2020) 1128–1135.
[130] G. Li, S. Liu, Z. Liu, Y. Zhao, High interfacial-energy and lithiophilic Janus interphase enables stable lithium metal anodes, Small 17 (2021) e2102196.
[131] W. Lu, L. Sun, Y. Zhao, T. Wu, L. Cong, J. Liu, Y. Liu, H. Xie, Elongating the cycle life of lithium metal batteries in carbonate electrolyte with gradient solid electrolyte interphase layer, Energy Stor. Mater. 34 (2021) 241–249.
[132] L. Su, H. Charalambous, Z. Cui, A. Manthiram, High-efficiency, anode-free lithium–metal batteries with a close-packed homogeneous lithium morphology, Energy Environ. Sci. 15 (2022) 843–854.
[133] J. Wu, C. Lin, Q. Liang, G. Zhou, J. Liu, G. Liang, M. Wang, B. Li, L. Hu, F. Ciucci, Q. Liu, G. Chen, X. Yu, Sodium-rich NASICON structured cathodes for boosting the energy density and lifespan of sodium-free-anode sodium metal batteries, InfoMat 4 (2022) e12288.
[134] X. Zeng, M. Mahato, W. Oh, H. Yoo, V.H. Nguyen, S. Oh, G. Valurouthu, S.K. Jeong, C.W. Ahn, Y. Gogotsi, I.K. Oh, Stoichiometric $Ti_3C_2T_x$ coating for inhibiting dendrite growth in anode-free lithium metal batteries, Energy Environ. Mater. 7 (2024) e12686.
[135] Y. Tian, Y. An, C. Wei, H. Jiang, S. Xiong, J. Feng, Y. Qian, Recently advances and perspectives of anode-free rechargeable batteries, Nano Energy 78 (2020) 105344.
[136] Z. Li, X. Huang, L. Kong, N. Qin, Z. Wang, L. Yin, Y. Li, Q. Gan, K. Liao, S. Gu, T. Zhang, H. Huang, L. Wang, G. Luo, X. Cheng, Z. Lu, Gradient nano-recipes to guide lithium deposition in a tunable reservoir for anode-free batteries, Energy Stor. Mater. 45 (2022) 40–47.
[137] Y. Lin, T. Wang, L. Zhang, X. Peng, B. Huang, M. Wu, T. Zhao, In-situ forming lithiophilic-lithiophobic gradient interphases for dendrite-free all-solid-state Li metal batteries, Nano Energy 99 (2022) 107395.
[138] L. Xiang, D.C. Jiang, Y. Gao, C.F. Zhang, X.D. Ren, L.Y. Zhu, S. Gao, X.W. Zhan, Self-formed fluorinated interphase with Fe valence gradient for dendrite-free solid-state sodium–metal batteries, Adv. Funct. Mater. 34 (2024) 2301670.
[139] J. Xing, W. Fan, J. Li, Z. Wang, Z. Wei, Y. Zhao, Orientation gradient architecture of nanofibrous separator towards mechanical enhancement and ion transport acceleration for lithium-ion batteries, Electrochim. Acta 441 (2023) 141794.
[140] Y. Lai, Y. Zhao, W. Cai, J. Song, Y. Jia, B. Ding, J. Yan, Constructing ionic gradient and lithiophilic interphase for high-rate Li-metal anode, Small 15 (2019) e1905171.
[141] Z. Sun, H. Jin, Y. Ye, H. Xie, W. Jia, S. Jin, H. Ji, Guiding sodium deposition through a sodiophobic–sodiophilic gradient interfacial layer for highly stable sodium metal anodes, ACS Appl. Energy Mater. 4 (2021) 2724–2731.
[142] H.J. Noh, M.H. Lee, B.G. Kim, J.H. Park, S.M. Lee, J.H. Choi, 3D carbon-based porous anode with a pore-size gradient for high-performance lithium metal batteries, ACS Appl. Mater. Interfaces 13 (2021) 55227–55234.
[143] S.H. Hong, D.H. Jung, J.H. Kim, Y.H. Lee, S.J. Cho, S.H. Joo, H.W. Lee, K.S. Lee, S.Y. Lee, Electrical conductivity gradient based on heterofibrous scaffolds for stable lithium–metal batteries, Adv. Funct. Mater. 30 (2020) 1908868.
[144] Y.X. Zhan, P. Shi, R. Zhang, X.Q. Zhang, X. Shen, C.B. Jin, B.Q. Li, J.Q. Huang, Deciphering the effect of electrical conductivity of hosts on lithium deposition in composite lithium metal anodes, Adv. Energy Mater. 11 (2021) 2101654.
[145] X. He, Y. Ni, Y. Li, H. Sun, Y. Lu, H. Li, Z. Yan, K. Zhang, J. Chen, An MXene-based metal anode with stepped sodiophilic gradient structure enables a large current density for rechargeable Na-O_2 batteries, Adv. Mater. 34 (2022) e2106565.
[146] K. Tantratian, D. Cao, A. Abdelaziz, X. Sun, J. Sheng, A. Natan, L. Chen, H. Zhu, Stable Li metal anode enabled by space confinement and uniform curvature through lithiophilic nanotube arrays, Adv. Energy Mater. 10 (2019) 1902819.
[147] L. Zhang, H. Zheng, B. Liu, Q. Xie, Q. Chen, L. Lin, J. Lin, B. Qu, L. Wang, D.-L. Peng, Homogeneous bottom-growth of lithium metal anode enabled by double-gradient lithiophilic skeleton, J. Energy Chem. 57 (2021) 392–400.
[148] Z. Xiao, Y.-N. Zhou, X. Wang, J. Cui, M. Yang, C. Shu, D. Han, J. Zhou, C. Peng, W. Tang, Y. Wu, Dual-layered 3D composite skeleton enables spatially ordered lithium plating/stripping for lithium metal batteries with ultra-low N/P ratios, ACS Appl. Energy Mater. 5 (2022) 14071–14080.
[149] Y. Zhang, M. Yao, T. Wang, H. Wu, Y. Zhang, A 3D hierarchical host with gradient-distributed dielectric properties toward dendrite-free lithium metal anode, Angew. Chem. Int. Ed. 63 (2024) e202403399.
[150] Y. Xu, C. Wang, E. Matios, J. Luo, X. Hu, Q. Yue, Y. Kang, W. Li, Sodium deposition with a controlled location and orientation for dendrite-free sodium metal batteries, Adv. Energy Mater. 10 (2020) 2002308.
[151] Y.C. Liu, B.Y. Yuan, C. Sun, Y.H. Lu, X.P. Lin, M.H. Chen, Y.S. Xie, S.Q. Zhang, C. Lai, Ultralow-expansion lithium metal composite anode via gradient framework design, Adv. Funct. Mater. 32 (2022) 2202771.
[152] X. Zhang, J. Li, K. Qi, Y. Yang, D. Liu, T. Wang, S. Liang, B. Lu, Y. Zhu, J. Zhou, An ion-sieving Janus separator toward planar electrodeposition for deeply rechargeable Zn-metal anodes, Adv. Mater. 34 (2022) e2205175.
[153] J.H. Kwak, S. Park, S. Shin, S. Park, C. Kang, S.-H. Yu, J. Moon, H.-D. Lim, Geometrical design of top-to-bottom magnesiophilicity-gradient host for reversible Mg-metal batteries, Energy Stor. Mater. 59 (2023) 102762.
[154] S. Wang, Y. Guo, X. Du, L. Xiong, Z. Huang, X. Li, M. Ma, Z. Liang, Y. Xie, Space limited growth strategy for ultra-high areal capacity rechargeable aluminum batteries, Energy Storage Mater. 60 (2023) 102826.
[155] J. Bi, Y. Liu, Z. Du, K. Wang, W. Guan, H. Wu, W. Ai, W. Huang, Bottom-up magnesium deposition induced by paper-based triple-gradient scaffolds toward flexible magnesium metal batteries, Adv. Mater. 36 (2023) e2309339.
[156] Y. Gao, Q. Cao, J. Pu, X. Zhao, G. Fu, J. Chen, Y. Wang, C. Guan, Stable Zn anodes with triple gradients, Adv. Mater. 35 (2023) e2207573.
[157] Q. Cao, Y. Gao, J. Pu, X. Zhao, Y. Wang, J. Chen, C. Guan, Gradient design of imprinted anode for stable Zn-ion batteries, Nat. Commun. 14 (2023) 641.
[158] Y. Wu, X. Wang, F. Zhang, L. Hai, Q. Chen, C. Chao, A. Yang, Y. Sun, D. Jia, Combining Janus separator and organic cathode for dendrite-free and high-performance Na-organic batteries, Adv. Funct. Mater. 34 (2023) 2309552.
[159] P. Zhai, N. Ahmad, S. Qu, L. Feng, W. Yang, A lithiophilic–lithiophobic gradient solid electrolyte interface toward a highly stable solid-state polymer lithium metal batteries, Adv. Funct. Mater. 34 (2024) 2316561.
[160] H. Yang, W. Jia, J. Zhang, Y. Liu, Z. Wang, Y. Yang, L. Feng, X. Yan, T. Li, W. Zou, J. Li, Gradient three-dimensional current collector with lithiophilic nanolayer regulation for efficient lithium metal anode construction, J. Colloid Interface Sci. 661 (2024) 870–878.
[161] Z. Zhu, Z. Liu, R. Zhao, X. Qi, J. Ji, F. Yang, L. Qie, Y. Huang, Heterogeneous nitride interface enabled by stepwise-reduction electrolyte design for dense Li deposition in carbonate electrolytes, Adv. Funct. Mater. 32 (2022) 2209384.
[162] J. Zhou, F. Wu, G. Wei, Y. Hao, Y. Mei, L. Li, M. Xie, R. Chen, Lithium-metal host anodes with top-to-bottom lithiophilic gradients for prolonged cycling of rechargeable lithium batteries, J. Power Sources 495 (2021) 229773.
[163] X. Zhou, Q. Zhang, Z. Zhu, Y. Cai, H. Li, F. Li, Anion-reinforced solvation for a gradient inorganic-rich interphase enables high-rate and stable sodium batteries, Angew. Chem. Int. Ed. 61 (2022) e202205045.